

ON THE ABSENCE OF WIND SIGNATURES IN GRB AFTERGLOW SPECTRA: CONSTRAINTS ON THE WOLF-RAYET WINDS OF GRB PROGENITORS

HSIAO-WEN CHEN¹, JASON X. PROCHASKA², ENRICO RAMIREZ-RUIZ^{2,3}, JOSHUA S. BLOOM^{4,5}, MIROSLAVA DESSAUGES-ZAVADSKY⁶, AND RYAN J. FOLEY⁴

Accepted for Publication in the Astrophysical Journal

ABSTRACT

We investigate available constraints on the circumstellar medium (CSM) around long-duration γ -ray burst (GRB) progenitors from afterglow spectra. We first establish a statistical sample of five GRB afterglow spectra that have been collected and analyzed with no prior knowledge of the line-of-sight properties. This sample is then adopted for a uniform search of Wolf-Rayet wind signatures, as represented by CIV $\lambda\lambda$ 1548, 1550 absorption doublets at $\Delta v = -1000$ to -5000 km s⁻¹ from the GRBs (hereafter CIV₁₅). We report the detection of a single CIV₁₅ absorber at $\Delta v \approx -1500$ km s⁻¹ from GRB 050730 and none in the rest. Our search yields an estimate of 20% for the incidence of CIV₁₅ absorbers with rest-frame absorption equivalent width EW(CIV 1548) > 0.2 Å near GRB host galaxies, consistent with the incidence of intergalactic CIV₁₅ near classical damped Ly α absorbers toward quasar sightlines. Including the two CIV₁₅ absorbers previously known toward GRB 021004, we further demonstrate that the presence of H⁰, C⁺, and Si⁺ together with the absence of excited C⁺ or Si⁺ argue against a CSM origin. The null result is consistent with the expectation that the circumburst medium is fully ionized by the afterglow radiation field. We examine possible scenarios for the survival of the C³⁺ ions, including a clumpy wind model. We find that a clumpy wind is unable to effectively shield the ionizing radiation and allow C³⁺ to survive at $r < 10$ pc from the afterglow. We conclude that the lack of CSM-originated CIV₁₅ absorbers is consistent with Wolf-Rayet winds terminating at < 30 pc from their progenitor stars.

Subject headings: gamma rays: bursts—ISM: abundances—ISM: kinematics—intergalactic medium

1. INTRODUCTION

A massive star origin of most long-duration, soft-spectrum γ -ray bursts (GRBs) has now been well-established on empirical grounds (see Woosley & Bloom 2006 for a recent review). Not only the locations of these GRBs trace closely the spatial distribution of young stars in their host galaxies (e.g. Bloom, Kulkarni, & Djorgovski 2002, Hammer et al. 2006; Fruchter et al. 2006), but a growing number of afterglows are also observed to exhibit spectral features that are characteristic of a core-collapse supernova (Hjorth et al. 2003; Stanek et al. 2003; but see Fynbo et al. 2006a, Gal-Yam et al. 2006, & Della Valle et al. 2006). In the popular collapsar model, likely candidate progenitors of long-duration GRBs are Wolf-Rayet stars that undergo a significant mass loss through stellar winds (MacFadyen & Woosley 1999). It is therefore expected that the circumstellar medium (CSM) has been regulated by the ejected wind material throughout the lifetime of the progenitor star (Wijers 2001; Ramirez-Ruiz et al. 2001; Chevalier et al. 2004; Ramirez-Ruiz et al. 2005; van Marle et al. 2005; Eldridge et al. 2006; van Marle et al. 2006).

In principle, the presence of Wolf-Rayet winds in the circumburst medium can be demonstrated in an early-

time, single-epoch afterglow spectrum. Specifically, ultraviolet spectra of local Wolf-Rayet stars exhibit prominent P-cygni profiles in N V λ 1242, Si IV λ 1442, and CIV λ 1550 transitions (e.g. Niedzielski & Rochowicz 1994; Willis et al. 2004) that indicate a wind terminal velocity up to $v_{\text{term}} = 5000$ km s⁻¹ (Figure 1). Numerical simulations of single stars show that a free-expanding wind will imprint a narrow absorption-line component in the afterglow spectrum, blue-shifted ($\Delta v \lesssim -1000$ km s⁻¹) from the host redshift (van Marle, Langer, & García-Segura 2005). Such blue-shifted, high-velocity absorption components have been reported in CIV transitions for GRB 021004 at $z_{\text{GRB}} = 2.329$ (Møller et al. 2002; Mirabal et al. 2003; Schaefer et al. 2003; Fiore et al. 2005; Fynbo et al. 2005; Starling et al. 2005; see also Lazzati et al. 2006), GRB 030226 (Klose et al. 2004), and GRB 050505 at $z_{\text{GRB}} = 4.2741$ (Berger et al. 2006), but the origin of these high-velocity CIV absorption components is ambiguous for three main reasons.

First, over a large velocity interval, between $\Delta v = 1000$ and $\Delta v = 5000$ km s⁻¹ *blueward* of the host redshift, the likelihood of finding an intervening absorber originated in a foreground galaxy along the line of sight is non-negligible. Second, the presence of an intense ultraviolet radiation field from the optical afterglow substantially increases the ionization of the circumburst medium. It therefore prohibits most ions from surviving at ≤ 30 pc radius from the afterglow. A CSM origin of these absorbers would require the Wolf-Rayet winds to reach beyond 30 pc, but observations of local Wolf-Rayet stars show that the wind blown bubbles have a typical size of < 10 pc (Gruendl et al. 2000). Finally, the circumburst medium is expected to be highly ionized even at > 30 pc, due to the presence

¹Department of Astronomy & Astrophysics, University of Chicago, Chicago, IL 60637, hchen@oddjob.uchicago.edu

²UCO/Lick Observatory; University of California, Santa Cruz, Santa Cruz, CA 95064, xavier@ucolick.org

³Institute for Advanced Study, Olden Lane, Princeton, NJ 08540

⁴Department of Astronomy, 601 Campbell Hall, University of California, Berkeley, CA 94720 jlbloom@astron.berkeley.edu

⁵Sloan Research Fellow

⁶Observatoire de Genève, 51 Ch. des Maillettes, 1290 Sauverny, Switzerland

of the intense afterglow radiation field. But the observed CIV abundance alone is insufficient for constraining the ionization state of the gas around the afterglow. A full consideration of all species at different ionization stages is necessary (e.g. Fynbo et al. 2005).

We have established a statistical sample of five GRB afterglows for which the afterglow spectra were collected and analyzed with no prior knowledge of the absorption-line properties along the line of sight. We have also assembled an early sample of previous GRB afterglows for which the spectra are available to us. The statistical sample allows an unbiased estimate of the incidence of the blue-shifted, high-velocity CIV absorption components. The statistical sample and early sample together allow us to investigate the nature of the blue-shifted, high-velocity CIV absorption components based on a suite of ionization models. In § 2, we present the GRB samples and summarize the available spectroscopic data for each burst. In § 3, we examine the possible intergalactic nature of these CIV absorbers based on the relative abundances between different ionization states of carbon and silicon. In § 4, we consider the afterglow radiation field estimated from light-curve observations, and constrain the extent of Wolf-Rayet winds based on the presence and absence of high-velocity CIV absorbers in the afterglow spectra. We further discuss the scenarios that will allow C^{3+} to survive the intense afterglow radiation field. Finally, we summarize our study in § 5.

2. THE GRB SAMPLES

We have compiled a *statistical sample* of GRB sightlines for which we resolve the CIV $\lambda\lambda 1548, 1550$ absorption doublet (i.e. a spectral resolution $\delta v < 180 \text{ km s}^{-1}$) at signal-to-noise ratios of $S/N > 7$ per resolution element so that the CIV $\lambda 1548$ transition would be observed at $> 3\sigma$ confidence level to an EW limit of 0.4 \AA over a 170 km s^{-1} velocity interval. The GRB sightlines in this sample are selected entirely based on the data quality (spectral resolution δv and S/N) from the GRAASP¹ database with no prior knowledge of the presence or absence of intervening absorbers. These include GRBs 050730, 050820, 050908, 051111, and 060418, and form a statistically unbiased sample for a blind search of intervening CIV absorbers.

In addition, we examine the GRB spectra that are available in the literature, in search of Wolf-Rayet signatures. These sightlines, despite incomplete and biased by known light-of-sight properties, offer additional insights for constraining the Wolf-Rayet nature of GRB progenitor stars. The GRBs in this category are GRBs 000926, 021004, and 030323. We call this an “early sample”, because the events occurred prior to 2004.

In both the *statistical* and the *early* samples, we search for blue-shifted, high-velocity components of CIV within $|\Delta v| \leq v_{\text{term}} \text{ km s}^{-1}$ in the afterglow spectra. The velocity threshold v_{term} is chosen to match the terminal velocity observed for galactic Wolf-Rayet stars (Figure 1). Based on 131 objects in the VIIth catalogue of galactic Wolf-Rayet stars by van der Hucht (2001), we show that all have a terminal wind velocity of $\leq 5000 \text{ km s}^{-1}$. The search of high-velocity CIV components is therefore carried out at $|\Delta v| < v_{\text{term}} = 5000 \text{ km s}^{-1}$. An additional selection

threshold for $\Delta v = -1000 \text{ km s}^{-1}$ is applied based on the maximum velocity of galactic winds observed in starburst galaxies at $z > 1$ (e.g. Adelberger et al. 2005). The nature of CIV within $\Delta v > -1000 \text{ km s}^{-1}$ becomes more ambiguous due to possibility of a large-scale galactic wind. We therefore exclude this region from consideration.

The blue-shifted, high-velocity CIV absorbers identified over the velocity interval of $-5000 \leq \Delta v \leq -1000 \text{ km s}^{-1}$ (hereafter designated as CIV₁₅) from the GRB host redshift z_{GRB} represent likely wind signatures of the progenitor stars. We also search for the presence of C II, Si II, Si IV, and additional ions whenever the transitions are covered. These additional transitions are crucial for constraining the ionizing radiation field around the absorbing gas. Here we summarize available spectroscopic data and our search results. For each source, the zero relatively velocity $\Delta v = 0$ corresponds to the redshift of the afterglow, which is determined based on the absorption profiles of low-ionization transitions such as C II, Si II, Al II, and Fe II.

2.1. The Statistical Sample

2.1.1. GRB 050730 at $z = 3.96855$

This GRB was first discovered by the Swift satellite on UT 2005 July 30 (Holland et al. 2005). An optical source was found promptly using the Ultraviolet-Optical Telescope (UVOT) on board Swift with $V = 17.6$ about three minutes after the burst trigger (Holland et al. 2005). This source was subsequently noted by Cobb & Bailyn (2005) to fade, confirming it as the optical afterglow. We obtained an echelle spectrum of the afterglow, using the MIKE spectrograph (Bernstein et al. 2003) on the Magellan Clay telescope, four hours after the initial trigger. Descriptions of the data were presented in Chen et al. (2005) and Prochaska et al. (2006). The spectrum covers a full spectral range from 3300 \AA through 9400 \AA with a spectral resolution of $\delta v \approx 10 \text{ km s}^{-1}$ at wavelength $\lambda = 4500 \text{ \AA}$ and $\delta v \approx 12 \text{ km s}^{-1}$ at $\lambda = 8000 \text{ \AA}$. The host of the GRB exhibits a strong damped Ly α absorption feature with $\log N(\text{H I}) = 22.15 \pm 0.05$, and abundant heavy ions with $> 95\%$ of the absorption confined within $-200 \leq \Delta v \leq 50 \text{ km s}^{-1}$.

Figure 2 shows the absorption-line profiles of CIV $\lambda\lambda 1548, 1550$, Si IV $\lambda\lambda 1393, 1402$, C II $\lambda 1334$, and Si II $\lambda 1526$ observed in the host ISM. The spectral region near the CIV absorption doublet is contaminated by the atmosphere A-band absorption forest, but we identify a CIV₁₅ absorber at $\Delta v = -1500 \text{ km s}^{-1}$. Comparison with a quasar spectrum obtained using the same instrument at the same site (shown as the magenta curve in Figure 2) confirms the lack of atmosphere absorption transition at the location of these CIV₁₅ lines. The identification is further supported by a consistent kinematic profile of the Si IV $\lambda\lambda 1393, 1402$ doublet transitions, for which we measure $\log N(\text{Si IV}) = 13.9 \pm 0.1$. For the CIV transitions, we measure a lower limit to the rest-frame absorption equivalent width of $\text{EW}(\lambda 1550) \geq 0.36 \text{ \AA}$. At this redshift, the C II $\lambda 1334$ transition is contaminated by a pair of CIV absorption doublet at lower redshifts, $z = 3.254$ and $z = 3.258$. Therefore, no constraints can be obtained. We do, however, identify weak Si II $\lambda 1526$ absorption and a strong Si II $\lambda 1260$ profile.

¹<http://www.graasp.org/>

2.1.2. GRB 050820A at $z = 2.6147$

This GRB was first discovered by the Swift satellite on UT 2005 August 20 (Page et al. 2005). An optical transient, reported less than 1 hour after the GRB, was identified in data taken shortly after the trigger (Fox & Cenko 2005; Vestrand et al. 2006). We obtained an echelle spectrum of the afterglow, using the HIRES (Vogt et al. 1994) on the Keck I telescope, an hour after the initial trigger. Descriptions of the data were presented in Prochaska et al. (2006). The spectrum covers a full spectral range from 3800 Å through 8000 Å with a spectral resolution of $\delta v \approx 7.5 \text{ km s}^{-1}$ across the entire spectral range. The host of the GRB exhibits a strong damped Ly α absorption feature with $\log N(\text{H I}) = 21.0 \pm 0.1$, and abundant heavy ions with $> 95\%$ of the absorption confined within $-250 \leq \Delta v \leq 200 \text{ km s}^{-1}$.

Figure 3 shows the absorption-line profiles of C IV $\lambda\lambda$ 1548, 1550, Si IV $\lambda\lambda$ 1393, 1402, C II λ 1334, Si II λ 1260, and Al II λ 1670 observed in the host ISM. While the host ISM shows complex, multiple-component absorption features at $|\Delta v| < 250 \text{ km s}^{-1}$ in C IV and Si IV transitions, it does not exhibit additional blue-shifted, high-velocity component beyond this velocity range at a $3\text{-}\sigma$ upper limit of $\text{EW}(\lambda 1548) = 0.2 \text{ Å}$ over $\delta v = 7.5 \text{ km s}^{-1}$.

2.1.3. GRB 050908 at $z = 3.344$

This GRB was discovered by the Swift satellite on UT 2005 September 8 (Goad et al. 2005). An optical transient, seen in data taken 14 minutes after the burst, was reported ≈ 80 minutes after the GRB trigger (Torii et al. 2005; see also Cenko et al. 2005 and Li et al. 2005). We obtained a low-resolution spectrum of the afterglow, using GMOS on the Gemini north telescope, four hours after the initial trigger (Foley et al. 2005). A moderate-resolution spectrum was taken four hours later by our group using DEIMOS (Faber et al. 2003) on the Keck II telescope (Prochaska et al. 2005). The final stacked GMOS spectrum covers a spectral range from 5073 Å through 7945 Å with chip gaps at 6006–6022 Å and 6972–6987 Å a spectral resolution of $\delta v \approx 200 \text{ km s}^{-1}$. The final stacked DEIMOS spectrum covers a spectral range from 6335 Å through 8960 Å with a spectral resolution of $\delta v \approx 40 \text{ km s}^{-1}$.

The GMOS spectrum covers the redshifted hydrogen Ly α λ 1215 transition. We measure $\log N(\text{H I}) = 19.2 \pm 0.2$. Figure 4 shows the absorption-line profiles of C IV $\lambda\lambda$ 1548, 1550, Si IV $\lambda\lambda$ 1393, 1402, C II λ 1334, Si II λ 1526, and Al II λ 1670 observed in the host ISM. The host galaxy also exhibits abundant heavy ions with $> 95\%$ of the absorption confined within $-300 \leq \Delta v \leq 200 \text{ km s}^{-1}$. We do not detect C IV₁₅ beyond this velocity range at a $3\text{-}\sigma$ upper limit of $\text{EW}(\lambda 1548) = 0.28 \text{ Å}$ over $\delta v = 40 \text{ km s}^{-1}$.

2.1.4. GRB 051111 at $z = 1.54948$

This GRB was discovered by the Swift satellite on UT 2005 November 11 (Sakamoto et al. 2005). An optical transient was found 27 s after the burst on the ground (Rykoff et al. 2005). An echelle spectrum was taken an hour after the initial burst by the Keck Observatory staff, using HIRES on the Keck I telescope. However, the echelle spectrum does not extend below 4000 Å, where the redshifted C IV absorption is expected. We also obtained a

low-resolution spectrum of the afterglow, using GMOS on the Gemini north telescope, 2.6 hours after the initial trigger. The final stacked GMOS spectrum covers a spectral range from 3800 Å through 4400 Å with a spectral resolution of $\delta v \approx 170 \text{ km s}^{-1}$. Figure 5 shows the absorption profiles of C IV $\lambda\lambda$ 1548, 1550, Si II λ 1526, and Al II λ 1670 observed in the host ISM. The host galaxy also exhibits abundant heavy ions with $> 95\%$ of the absorption confined within $-200 \leq \Delta v \leq 100 \text{ km s}^{-1}$. We do not detect C IV₁₅ beyond this velocity range at a $3\text{-}\sigma$ upper limit of $\text{EW}(\lambda 1548) = 0.37 \text{ Å}$ over $\delta v = 170 \text{ km s}^{-1}$.

2.1.5. GRB 060418 at $z = 1.4901$

This GRB was first discovered by the Swift satellite on UT 2006 April 18 (Falcone et al. 2006). A candidate optical afterglow, with $V = 14.5$ mag, was reported from VOT images taken starting 88 seconds after the trigger (Falcone et al. 2006). We obtained an echelle spectrum of the afterglow, using the MIKE spectrograph on the Magellan Clay telescope, 28 minutes after the initial trigger. Descriptions of the data were presented in Prochaska et al. (2006). The spectrum covers a full spectral range from 3500 Å through 9000 Å with a spectral resolution of $\delta v \approx 12 \text{ km s}^{-1}$ at wavelength $\lambda = 7000 \text{ Å}$. The host of the GRB exhibits abundant heavy ions with $> 95\%$ of the absorption confined within $-200 \leq \Delta v \leq 100 \text{ km s}^{-1}$.

Figure 6 shows absorption-line profiles of C IV $\lambda\lambda$ 1548, 1550, Si IV $\lambda\lambda$ 1393, 1402, C II λ 1334, Si II λ 1526 and Al II λ 1670 observed in the host ISM. Over the velocity interval from $\Delta v = -5000 \text{ km s}^{-1}$ through $\Delta v = -1000 \text{ km s}^{-1}$, we do not detect additional components at a $3\text{-}\sigma$ upper limit of $\text{EW}(\lambda 1548) = 0.36 \text{ Å}$ over a spectral resolution element of $\delta v = 12 \text{ km s}^{-1}$.

2.2. The Early Sample

We have searched C IV₁₅ along the sightlines toward GRB 000926 (Hurley et al. 2000; Harrison et al. 2001), GRB 021004 (Shirasaki et al. 2002; Holland et al. 2003), and GRB 030323 (Graziani et al. 2003; Gilmore et al. 2003), for which afterglow spectra are available to us. The afterglow spectrum of GRB 000926 was obtained using the Echelle Spectrograph and Imager (ESI; Sheinis et al. 2002) on the Keck II telescope (Castro et al. 2003). We found no C IV₁₅ at a $3\text{-}\sigma$ upper limit to the rest-frame absorption equivalent width $\text{EW}(\lambda 1548) = 0.35 \text{ Å}$ over a spectral resolution element of $\delta v = 66 \text{ km s}^{-1}$. The afterglow spectrum of GRB 030323 was obtained using the FORS2 spectrograph on the VLT/UT4 telescope (Vreeswijk et al. 2004). We found no C IV₁₅ at a $3\text{-}\sigma$ upper limit to $\text{EW}(\lambda 1548) = 0.04 \text{ Å}$ over a spectral resolution element of $\delta v = 143 \text{ km s}^{-1}$.

Afterglow spectra of GRB 021004 were obtained, using various spectrographs on multiple telescopes (Castander et al. 2002; Chornock & Filippenko 2002; Salamanca et al. 2002; Castro-Tirado et al. 2002; Møller et al. 2002; Fiore et al. 2005; Starling et al. 2005). The host of this GRB does not exhibit a prominent damped Ly α absorption feature that is commonly seen in most GRB hosts (e.g. Vreeswijk et al. 2004; Chen et al. 2005; Berger et al. 2006; Jakobsson et al. 2006). Based on the Lyman limit absorption discontinuity and the observed absorption strength of

the Ly β transition, Fynbo et al. (2005) estimated a neutral hydrogen column density of $\log N(\text{H I}) = 19.5 \pm 0.5$. In addition, available echelle spectra of the optical afterglow clearly resolve two C IV $_{15}$ absorption components approaching $\Delta v = -3000 \text{ km s}^{-1}$. While a blue-shifted, high-velocity component is expected in the circumstellar medium of a Wolf-Rayet progenitor, the presence of two components is difficult to explain under the free-expanding wind model of a single progenitor star (e.g. van Marle et al. 2005).

We retrieved from the ESO Science Archive (program ID's 70.A-0599(B) and 70.D-0523(D)) echelle spectra of the source obtained 13.5 hours after the burst, using the Ultraviolet-Visual Echelle Spectrograph (UVES; D'Odorico et al. 2000) on the VLT Kueyen telescope. We examined and reduced the individual spectra. The data were weighted by their S/N ratios and co-added to form a final stacked spectrum. The final, stacked spectrum spanned a spectral range from 4200 to 9900 Å with a spectral resolution of $\approx 3.8 \text{ km s}^{-1}$ per pixel, and achieved a signal-to-noise ratio of $S/N \approx 20$ per resolution element at around 5200 Å. A copy of a low-resolution spectrum that was obtained nearly 4 days after the GRB, using the Low Resolution Imaging Spectrograph (LRIS) on the Keck I telescope was kindly made available to us by N. Mirabal. The spectrum covers the spectral range around the redshifted Ly α transition at the host redshift and has a spectral resolution of $\approx 150 \text{ km s}^{-1}$ per pixel. Descriptions of the LRIS observations are presented in Mirabal et al. (2003).

We present in Figure 7 the absorption-line profiles of H I Ly α λ 1215, C IV $\lambda\lambda$ 1548, 1550, Si IV $\lambda\lambda$ 1393, 1402, C II λ 1334, Si II λ 1526, and Al II λ 1670 observed in the host of GRB 021004. Figure 7 shows that in addition to the main absorption component at $|\Delta v| < 400 \text{ km s}^{-1}$ two absorption components are seen blue-shifted from the host redshift at $|\Delta v| = 2700$ (Component 1) and 2900 km s^{-1} (Component 2), respectively. A strong Ly α absorption feature is present at the location of the two blue-shifted, high-velocity C IV components, but not resolved in the LRIS spectrum. Mirabal et al. reported a rest-frame absorption equivalent width of $\text{EW}(\text{Ly}\alpha) = 3.9 \pm 0.6 \text{ Å}$, which implies a total neutral hydrogen column density² of $\log N(\text{H I}) \sim 19.5$ for a typical Doppler parameter of $b = 20 \text{ km s}^{-1}$. Our $N(\text{H I})$ estimate is consistent with that reported by Fynbo et al. (2005) from their HST observations of the Lyman limit discontinuity. We confirm this value with a Voigt profile fit to the LRIS data and estimate an uncertainty of 0.4 dex which is dominated by systematics (continuum fitting and line-blending). In addition to the strong H I Ly α transition, we also observe abundant low-ions such as C⁺ as evident by the C II λ 1334 transition at the location of Component 1.

We measure the ionic column density of each species using the apparent optical depth method (Savage & Sembach 1991). The measurements are presented in Table 1. The

²Mirabal et al. (2003) derived progressively larger $N(\text{H I})$, from $\log N(\text{H I}) = 14.95$ to $\log N(\text{H I}) = 16.11$, based on the observed $\text{EW}(\text{Ly}\alpha)$, $\text{EW}(\text{Ly}\beta)$, and $\text{EW}(\text{Ly}\gamma)$. These authors assumed that these transitions fall on the linear part of the curve of growth, but noted the differences in the derived $N(\text{H I})$ as suggestive of the lines being saturated. The difference between our derived $N(\text{H I})$ and those from Mirabal et al. arises entirely due to the assumption these authors adopted, which is invalid for saturated lines.

large contrast in the observed relative column densities of C⁺ and C³⁺ for components 1 and 2 suggests that they arise in distinct phases (see § 3.2). Furthermore, strong absorption from neutral hydrogen and low ionization species such as C⁺ strongly indicate that this absorber may not originate in the highly ionized circumstellar medium of the progenitor. We will discuss various ionization scenarios in § 3.2.

3. THE NATURE OF BLUE-SHIFTED, HIGH-VELOCITY CIV ABSORBERS

Our systematic search for C IV $_{15}$ absorbers along five GRB lines of sight in the *statistical sample* has yielded identifications of one absorber along the sightline toward GRB 050730 at $\Delta v \approx -1500 \text{ km s}^{-1}$. Despite a heterogeneous spectral data set, our survey is sensitive to C IV $_{15}$ absorbers of rest-frame absorption equivalent width $\text{EW}(\lambda 1548) > 0.04 - 0.4 \text{ Å}$ at the $3\text{-}\sigma$ significant level, when scaled to a uniform $\delta v = 170 \text{ km s}^{-1}$ velocity resolution element. We estimate that the incidence of C IV $_{15}$ absorbers with $\text{EW}(\lambda 1548) > 0.4 \text{ Å}$ is 20% near a GRB afterglow.

Despite a small sample, we attempt to determine the confidence level of our estimate in the incidence of C IV $_{15}$ absorbers based on a bootstrap re-sampling analysis. We first adopt the five GRB sightlines as the parent sample. Then we randomly select five fields from the parent sample, allowing for duplication. Next, we measure the incidence of C IV $_{15}$ absorbers in the new sample. Finally, we repeat the procedure 1000 times and measure the scatter in our measurements. Our bootstrap analysis yields a 68% confidence interval of 0 – 40% in the incidence of C IV $_{15}$ absorbers with $\text{EW}(\lambda 1548) > 0.4 \text{ Å}$.

Including sources in the *early sample* from the literature (GRBs 000926, 021004, and 030323), we confirm additional two components along the sightline toward GRB 021004 at $\Delta v \approx -2800 \text{ km s}^{-1}$. We note that possible C IV $_{15}$ features have also been reported for GRB 030226 at $z_{\text{GRB}} = 1.986$ by Klose et al. (2004) and discussed by Shih et al. (2006). The high spectral resolution data are not accessible to us. The source is therefore not included in our analysis. A summary of the observed absorption line properties is presented in Table 2, where we list for each field the estimated isotropic energy release of γ -ray photons E_{iso} , the redshift of the GRB host, $N(\text{H I})$ and metallicity of the host ISM, the maximum velocity span of the observed blue-shifted C IV absorption doublet, and the time period when the afterglow spectra were obtained $t_{\text{obs}}^{\text{spec}}$. We find no correlation between the presence of C IV $_{15}$ and other factors, such as E_{iso} or $t_{\text{obs}}^{\text{spec}}$.

While a Wolf-Rayet wind from the GRB progenitor is a natural candidate for explaining the observed C IV $_{15}$ absorbers, it is clear that the majority of GRB afterglow spectra do not exhibit these features. Here we investigate the nature of these C IV $_{15}$ clouds, taking into account the presence of ions at lower ionization stages.

3.1. The Likelihood of Contaminations by Intervening Absorbers at $z_{\text{abs}} < z_{\text{GRB}}$

We first consider the statistical sample of five GRB lines of sight as a whole and evaluate the likelihood of finding an intervening C IV $_{15}$ absorber over $|\Delta v| = 1000 - 5000$

km s^{-1} at $z_{\text{CIV}} < z_{\text{GRB}}$ based on known statistics from quasar absorption-line studies. A non-negligible probability of finding a foreground absorber over the redshift pathlength surveyed by this sample would challenge the validity of attributing these absorbers to the GRB host environment.

Random surveys toward quasar lines of sight have shown a mean number density per unit redshift interval of $n_{\text{CIV}}(z = 2) = 1.8 \pm 0.4$ for CIV absorbers of $\text{EW}(\lambda 1548) > 0.4 \text{ \AA}$ and $n_{\text{CIV}}(z = 2) \sim 5$ for $\text{EW}(\lambda 1548) > 0.15 \text{ \AA}$ (Steidel 1992). The total redshift pathlength over $\Delta v = 1000 - 5000 \text{ km s}^{-1}$ along the GRB lines of sight in our sample of five is $\Delta z = 0.23$. Therefore, the probability of detecting at least one random CIV absorber of $\text{EW}(\lambda 1548) > 0.4$ is 34%. At lower threshold $\text{EW}(\lambda 1548) > 0.15$, the probability of detecting at least one random absorber at lower redshifts is 64%. We note that the CIV₁₅ absorber toward GRB 050730 has $\text{EW}(\lambda 1548) > \text{EW}(\lambda 1550) \geq 0.36 \text{ \AA}$.

It is also necessary, however, to take into account the possibility of large-scale clustering between CIV absorbers through clustering of the absorbing galaxies. Galaxy clustering may be important in this analysis, particularly because the search is carried out near a GRB host galaxy. Unfortunately, the cross-correlation function of intervening CIV absorbers and GRB host galaxies is not well determined. Existing two-point correlation measurements are for CIV absorbers of a wide range of observed column density (e.g. Petitjean & Bergeron 1994). These are likely underestimates of the clustering extent and amplitude for strong CIV absorbers, because stronger absorbers are expected to cluster more strongly with one another (Adelberger et al. 2005).

As a first estimate, we have searched a sample of 53 quasar sightlines from the Keck/UCSD High Resolution database (Prochaska et al. 2007) with known intervening super Lyman limit systems (SLLS) of $\log N(\text{H I}) > 19$ or damped Ly α absorbers (DLAs) of $\log N(\text{H I}) \geq 20.3$ (comparable to the $N(\text{H I})$ found in GRB host galaxies) at $1.7 < z_{\text{abs}} < 4.3$. The DLAs are believed to trace the majority of the galactic population at $z > 2$. Although their luminosity (or mass) function has not been established empirically, current expectation is that a significant fraction correspond to sub- L_* galaxies (e.g. Weatherley et al. 2005) similar to GRB host galaxies (e.g. Christensen, Hjorth, & Gorosabel 2004).

We searched for CIV₁₅ absorbers in the vicinity ($-5000 \text{ km s}^{-1} \leq \Delta v \leq -1000 \text{ km s}^{-1}$) of intervening DLAs toward background quasars (Figure 8). This QSO-DLA sample serves as a control sample for estimating the statistical significance of possible “over-abundance” of CIV₁₅ absorbers in the vicinity of GRB host galaxies. In the sample of 53 DLAs identified along quasar sightlines, we find a total of six CIV₁₅ absorbers to an EW limit of 0.2 \AA near five DLAs. Therefore, the incidence of CIV₁₅ from a DLA is ≈ 0.11 . Namely, there is on average one CIV₁₅ absorber in the vicinity of every nine DLAs. Adopting this expectation, we estimate that the probability of detecting at least one CIV₁₅ absorber near a GRB host galaxy in our *statistical sample* of five GRBs is 42%. While the sample of GRB host galaxies is still small, our exercise shows that the probability for the CIV₁₅ absorber toward GRB 050730 to originate in a foreground galaxy at $z < z_{\text{GRB}}$ is non-

negligible.

3.2. Constraints from the Absence of Excited Ions

A nearly generic feature in the afterglow spectra of the ISM surrounding the GRB is the presence of the fine-structure absorption of C^+ , Si^+ , O^0 and Fe^+ (e.g. Chen et al. 2005; Berger et al. 2006; Fynbo et al. 2006). While these lines were initially interpreted as signatures of a high density, circumstellar medium, Prochaska, Chen, & Bloom (2006; hereafter PCB06) demonstrated that indirect UV pumping would dominate the excitation if the gas is at $r \lesssim 100 \text{ pc}$ of the afterglow. Therefore, the presence or absence of absorption due to excited ions constrains the distance of the gas from the GRB event (see also Shin et al. 2006; Vreeswijk et al. 2006).

We examine the velocity profiles of various ions associated with the CIV₁₅ absorbers from GRB 021004 and from GRB 050730 (Figure 9). We include the low-ionization transitions of C II $\lambda 1334$ and Si II $\lambda 1260$ for GRB 021004 and GRB 050730, respectively, together with their associated fine-structure transitions. Both C^+ and Si^+ have a $J = 1/2$ ground-state and a corresponding $J = 3/2$ excited fine-structure level. It is clear that the ground-state is significantly populated for Component 1 of GRB 021004 and for the majority of the line-profile for GRB 050730. We set upper limits to the ratio of the excited to ground level $f \equiv N_{J=3/2}/N_{J=1/2}$ of $f < 0.05$ for Component 1 of GRB 021004 and $f < 0.1$ for GRB 050730. Although optical depth effects will generally imply $f < 1$ (PCB06), the very low f values require the gas lay at large distance from the GRB afterglow.

A lower limit to the distance of the gas from the afterglow can be obtained by calculating the total number of excitations from the afterglow prior to the onset of the spectroscopic observations, $t_{\text{obs}}^{\text{spec}}$. For both of these GRBs, we can neglect de-excitations from spontaneous decay because the lifetimes of the excited levels are considerably longer than $t_{\text{obs}}^{\text{spec}}$. Similarly, if the electron density of the gas were sufficient to collisionally de-excite the states, one would predict $f \gg 0.1$ (Silva & Viegas 2000). Adopting GRB 021004 as an example, we find from Figure 12 that the optical afterglow light curve is very complicated for this GRB (e.g. Pandey et al. 2003; Bersier et al. 2003). We therefore derive a spline-fit model of the empirical R_C -band measurements reported by Holland et al. (2003) and Uemura et al. (2003). In addition, we assume that $F_\nu \propto \nu^\beta$ with $\beta = -1$ noting that our calculation is not sensitive to this choice. We must also model the absorption line-profile of the gas ‘cloud’ to determine the number of photons absorbed prior to the onset of our spectroscopic observations. A single absorber with column density $N(\text{CII}) = 10^{14.5} \text{ cm}^{-2}$ and a Doppler parameter $b = 10 \text{ km s}^{-1}$ is a conservative approximation to the observed line-profile (the equivalent width actually underestimates the observed value). In the following, we only consider the C II $\lambda\lambda 1036$ and 1334 transitions.

The number of photons absorbed from ions in the ground-state of C^+ prior to spectroscopic observations is estimated by integrating over the light curve from $t_i = 1000 \text{ s}$ to $t_{\text{obs}}^{\text{spec}}$. We choose $t_i = 1000 \text{ s}$ because the light curve is not well defined prior to this time and to give a more conservative estimate of the photon number. Integrating to $t_i = 0 \text{ s}$

would likely increase the photon number by $< 30\%$. We find a photon surface density at distance r from the afterglow,

$$N_{\text{phot}} = 10^{18} \left(\frac{10 \text{ pc}}{r} \right)^2 \text{ cm}^{-2} . \quad (1)$$

While only a fraction of the excitations would be followed by a spontaneous decay to the $J = 3/2$ level in the ground term, a conservative estimate is 50%, because the upper level has a higher J value and correspondingly higher statistical weight. To set a lower limit to the distance of the gas from the afterglow, we calculate the distance at which the photon surface density matches twice the column density limit for the $J = 3/2$ level of C^+ as observed from the UVES observations, $N(\text{C II}^*) < 10^{13} \text{ cm}^{-2}$. This implies the gas occurs at a distance $r_{\text{min}} > 1 \text{ kpc}$ from the GRB afterglow. We derive a similar value for the Si^+ gas associated with GRB 050730.

The above argument is based primarily on the direct observations of the afterglow flux. No extrapolation is required for the prompt emission or to higher energies than observed for the afterglow radiation field. Furthermore, the conclusions are based on empirical observations of the abundances and are largely independent of shielding scenarios (which we will consider to explain the survival of C^{3+} ; § 4.3). This is understood by the fact that optical depth effects would yield excitation of C^+ in a thin layer of the gas facing the afterglow, producing a non-negligible amount of C II^* transitions. For example, in a layer of C^+ ions with $N(\text{C}^+) = 10^{13} \text{ cm}^{-2}$ where the C II transitions are optically thin, excited C^+ ions are expected to dominate but are absent in our data.

However, it is possible to design a scenario in which layers of high-column density gas absorb a large fraction of N_{phot} and are consequently photo-ionized by the afterglow just prior to $t_{\text{obs}}^{\text{spec}}$. This would require significant fine-tuning. Altogether, the absence of fine-structure absorption lends strong support for the conclusion that the C and Si ions identified at $v \approx 2800 \text{ km s}^{-1}$ and $v \approx 1500 \text{ km s}^{-1}$ toward GRB 021004 and GRB 050730, respectively, are not circumstellar material of the GRB progenitor.

3.3. Are the Absorbers Photo-ionized by the Metagalactic Radiation Field?

If the C IV_{15} absorbers found along the sightline toward GRB 021004 originate in foreground clouds at $z_{\text{C IV}} < z_{\text{GRB}}$, then these gaseous clouds are expected to be photo-ionized predominantly by the ultraviolet background radiation or possibly a local starburst (Simcoe 2006). Observations of abundance ratios between different ionization stages of a given species can be applied to constrain the ionization state of the gas.

We use the Cloudy software (Ferland et al. 1998; version 06.02) to calculate the expected population ratios between different ionization stages of carbon and silicon for clouds of plane parallel geometry and under photo-ionization equilibrium. We have assumed a metallicity of 0.1 solar and $\log N(\text{H I}) = 15$, appropriate for intervening, strong C IV absorbers along quasar lines of sight (e.g. Cowie et al. 1995). The results are not sensitive to the adopted metallicity and $N(\text{H I})$. We also note that the assumed solar relative abundances are not relevant because

we compare pairs of ions for the same elements³. Figure 10 shows the abundance ratios of C^+ to C^{3+} and Si^+ to Si^{3+} versus the ionization parameter $U \equiv \phi_{\gamma}/cn_{\text{H}}$, which represents the number of ionizing photons available per hydrogen particle.

Column density measurements presented in Table 1 for both high-velocity C IV components allow us to place limits on the ionization parameter. For component 1, $\text{C II } \lambda 1334$ is saturated. We can therefore place an upper limit at $\log U = -2.9$. For component 2, both C IV and Si IV are saturated. The $(\text{C II}/\text{C IV})$ and $(\text{Si II}/\text{Si IV})$ ratios yield a consistent lower limit of $\log U > -2.1$. We note that $\log U \lesssim -3$ is relatively low, even for Lyman limit systems (e.g. Bergeron & Stasínska 1986; Lopez et al. 1999; Chen & Prochaska 2000). On the other hand, the $\text{C II}/\text{C IV}$ ratio observed for the component 2 is typical of what is observed in the intergalactic medium (e.g. Songaila 2006).

The inferred limits for the ionization parameter U allow us to examine the gas properties of the absorbers. Adopting a meta-galactic radiation field of $J_{912} = 1.4 \times 10^{-21} \text{ erg s}^{-1} \text{ cm}^{-2} \text{ Hz}^{-1} \text{ sr}^{-1}$ measured at $z \sim 2$ (Scott et al. 2000), we derive a gas density of $n_{\text{H}} \sim 0.01 - 0.1 \text{ cm}^{-3}$ for $\log U = -2$ to $\log U = -3$. Comparisons between observations and expectations of photo-ionized gas in the intergalactic medium therefore demonstrate that the observed relative ionic abundances for the two C IV components can be naturally explained under a photo-ionization equilibrium with the meta-galactic radiation field. In particular, the upper limit on the ionization parameter for component 1 indicates that a higher gas density and lower ionization intensity is favored. Our photo-ionization analysis substantiates the fine-structure analysis from the previous section in that the gas is located at large distance from the GRB afterglow.

If we are to interpret the C IV_{15} absorption associated with GRB 021004 as intergalactic, then one might expect to identify a galaxy associated with this gas. Fynbo et al. (2005) find six faint sources in HST imaging in a $10'' \times 10''$ region around the host. This overdensity of faint objects is qualitatively consistent with the overabundance of Mg II absorbers at lower redshift along the sightline. Fiore et al. (2005) reported two groups of Mg II absorbers identified at $z = 1.380$ and $z = 1.602$ along the sightline (see also Prochter et al. 2006). Figure 11 shows these optical images obtained using HST/ACS with the F606W filter three days (left panel) and eight months (right panel) after the trigger. The images are retrieved from the HST data archive (Program ID = 9405). While the afterglow was still bright in the first epoch image, we point out a faint companion at an angular distance $\Delta\theta = 0.3''$ to the host galaxy, which corresponds to 2.5 kpc projected distance at $z = 2.299$. The host galaxy and the companion together within a $0.5''$ -radius aperture have a total brightness of $AB(\text{F606W}) = 24.55 \pm 0.05$ (Fynbo et al. 2005). We estimate that the companion contributes roughly 1/10 of the total flux and therefore has $AB(\text{F606W}) \approx 27.3$.

Recall that a $\text{Ly}\alpha$ absorption line with $\text{EW} = 3.9 \pm 0.6$

³Our analysis differs from those presented in Fiore et al. (2005) in two important aspects. First, we adopt only lower limits for saturated transitions. Second, we compare the same elements, but in different ionization stages. This is necessary due to potential biases imposed by different chemical abundance patterns in the CSM.

\AA is also identified at the location of the two CIV_{15} components (§ 2.2), although unresolved. The presence of $\text{Ly}\alpha$ absorber of $\log N(\text{H I}) = 19.5$ presents a further challenge to the origin of the absorber arising in the host environment. On the other hand, the $\text{Ly}\alpha$ absorption strength is consistent with originating in the extended gaseous halo of a faint dwarf galaxy at lower redshift (Chen et al. 2001). No deep image of the field around GRB 050730 has been reported yet.

4. IMPLICATIONS FOR THE CIRCUMSTELLAR MEDIUM OF GRB PROGENITOR STARS

The survey results from a statistical sample show that the majority of afterglow spectra do not exhibit expected wind signatures from Wolf-Rayet progenitors, consistent with the expectation that the circumburst medium is highly ionized. In addition, the fine-structure and photo-ionization analysis show that the known CIV_{15} absorbers near GRB afterglows most likely originate in a foreground galaxy along the sightline. Here we take into account the known radiation field from afterglow light-curve observations. The presence of wind signatures in an afterglow spectrum determines the minimum distance of the absorbing ions to the afterglow. The absence of wind signatures determines the maximum distance reached by the wind prior to the GRB phase, if the absence is due to photo-ionization of the wind. Considering a sample of afterglow spectra together allows us to estimate the typical extent of Wolf-Rayet winds. In the following discussion, we consider both smooth and clumpy media for allowing effective shielding of ionizing photons from the afterglow.

4.1. The Extent of Wolf-Rayet Wind around the Progenitor Stars

Figure 12 shows the optical light curves of four GRB afterglows in our spectroscopic sample, for which early-time (from < 10 minutes after the initial burst) photometric measurements are available. All but one of these afterglows reached an initial brightness of $R < 15.5$ mag and declined by 2 magnitudes in less than two hours (with the exception of GRB 021004). Even at $R = 17.5$, the corresponding intrinsic luminosity easily competes with the brightest quasars known at this redshift (see e.g. Fan et al. 2001). Despite a brief lifetime, the afterglow can easily ionize the circumstellar medium to large radii (see PCB06). The presence or absence of the CIV_{15} doublet features, coupled with the radiation field measured from afterglow observations, therefore, determines the extent of the Wolf-Rayet wind from the progenitor stars.

To assess the impact of the afterglow over the circumstellar medium, we estimate the number of ionizing photons released to the surrounding medium prior to the onset of the spectroscopic observations. We first adopt the afterglow of GRB 050820 as an example, given its well sampled optical light curve that shows both the prompt emission at $t_{\text{obs}} < t_{\text{GRB}} + 5$ min and afterglow radiation at later times (Vestrand et al. 2006). The transient nature of the afterglow indicates that accurate constraints on the ionization fraction of the surrounding medium require a time-dependent photo-ionization calculation (e.g. Perna & Lazzati 2002).

For an approximation of the ionization fraction of C^{3+} , however, we note that the recombination rate coefficient

$\alpha_R(\text{C}^{4+}) \sim 10^{-11.5} \text{ cm}^3 \text{ sec}^{-1}$ (Nahar & Pradhan 1997) at a gas temperature of $T \sim 10^{4-5} \text{ K}$ and electron density $n_e \sim 10^4 \text{ cm}^{-3}$, typical of a compact H II region, yields a characteristic recombination time scale

$$t_{\text{rec}}(\text{C}^{4+}) \sim 1 \text{ year} \gg t_{\text{obs}}^{\text{spec}}. \quad (2)$$

Since the timescale for observation ($< \text{a few hours}$ in the frame of the medium external to the GRB outflow) is much smaller than the recombination time for each GRB event (Table 2), the ionization fraction of the circumstellar medium can be approximated by considering only the amount of ionizing photons available to ionize C^{3+} .

For the afterglow of GRB 050820, we estimate an isotropic release of total ionizing photon number, $\phi_\gamma(h\nu \geq 64 \text{ eV}) \approx 1.8 \times 10^{60}$ over $\Delta t = t_{\text{obs}}^{\text{spec}} = 3240 \text{ s}$. Defining r_{min} as the radius of the ionization front where 99.99% of C^{3+} are ionized, we have $n(\text{C}^{3+})/n(\text{C}^{4+}) \approx 10^{-4}$ in an optically thin regime or

$$\frac{n(\text{C}^{3+})}{n(\text{C}^{4+})} = 10^{-4} = \exp \left[\frac{-\phi_\gamma \sigma_{ph}(\text{C}^{3+})}{4\pi r_{\text{min}}^2} \right]. \quad (3)$$

Therefore,

$$r_{\text{min}} = \left[\frac{\phi_\gamma \sigma_{ph}(\text{C}^{3+})}{1.1 \times 10^{39}} \right]^{1/2} \text{ pc}. \quad (4)$$

For $\sigma_{ph}(\text{C}^{3+}) = 6.6 \times 10^{-19} \text{ cm}^2$, we find that 99.99% of C^{3+} within 33 pc would be ionized. The lack of CIV_{15} in the spectrum is therefore consistent with the winds terminating at $< 30 \text{ pc}$ and becoming fully ionized shortly after the GRB event.

The afterglow spectrum of GRB 050820 presented in § 2.1.2 is sensitive to CIV transitions of $\log N_{2\sigma}(\text{CIV}) \geq 13.7$ at $\geq 2\text{-}\sigma$ significance level for a nominal Doppler parameter $b = 15 \text{ km s}^{-1}$. Therefore, it does not exclude the possibility that Wolf-Rayet winds with $\log N(\text{CIV}) < 13.7$ may be present at $r > r_{\text{min}}$. The lack of wind signatures in the host of GRB 050820 implies that if such winds exist and contain a large amount of C^{3+} ($\log N(\text{CIV}) > 13.7$) then it did not reach beyond 30 pc.

The presence of the two CIV_{15} components along the sightline toward GRB 021004 have been considered in the literature as the most likely candidate for Wolf-Rayet winds in the circumburst environment of GRBs, although our analyses in § 3 show that at least one (Component 1 at $\Delta v = -2675 \text{ km s}^{-1}$) is best-explained by a foreground cloud located at $> 1 \text{ kpc}$ from the afterglow and photo-ionized by the ultraviolet background radiation field.

Allowing the possibility for Component 2 at $\Delta v = -2900 \text{ km s}^{-1}$ to arise in the CSM of the progenitor star, we estimate the minimum radius for the C^{3+} ions to survive the afterglow radiation field. Adopting the total number of ionizing photons estimated by Lazzati et al. (2006) from both the prompt emission and the afterglow phase $\phi_\gamma = 4 \times 10^{60}$, we derive a minimum radius $r_{\text{min}} \sim 50 \text{ pc}$ according to Equation (4) and find that more than 99% of the C^{3+} ions are ionized within this radius⁴. Combining the upper limit derived for the extent of Wolf-Rayet

⁴This is a factor of three smaller than the distance of the CIV clouds derived by Lazzati et al. The difference is primarily due to a different ionization fraction adopted by these authors. Comparison between Equation (3) in the present paper and Equation (11) in Lazzati et al. shows that these authors have allowed the gas to be $\sim 60\%$ ionized when defining r_{min} . This leads to $r_{\text{min}} \sim 150 \text{ pc}$.

wind around the progenitor star of GRB 050820 (< 30 pc) with r_{\min} derived for GRB 021004, we find a maximum extent of 30 – 50 pc for the Wolf-Rayet winds around GRB progenitor stars.

4.2. Can the C^{3+} Ions Survive the Afterglow Radiation Field at $r < 30$ pc?

The large distance implied for the Wolf-Rayet winds of the progenitor of GRB 021004 from observations of Component 2 at $\Delta v = -2900$ km s $^{-1}$ is much larger than what is commonly observed for local Wolf-Rayet stars. The typical wind terminal shocks are found at $r \lesssim 10$ pc (García-Segura et al. 1996; Gruendl et al. 2000). In an effort to understand the physical conditions that determine the location of the wind terminal shock around a GRB progenitor star, van Marle et al. (2006) explored the parameter space spanned by the ISM density of the GRB host, the wind velocity, and the mass-loss rate during the Wolf-Rayet phase of the progenitor. According to their calculation, for the wind to reach beyond 50 pc at a wind-speed of $v_{WR} = 3000$ km s $^{-1}$ only a narrow parameter space is allowed. Their Figure 12 (van Marle et al. 2006) shows that a mass-loss rate of $1 \times 10^{-5} M_{\odot} \text{ yr}^{-1}$, an ISM density $\log \rho_{\text{ISM}} < -24$ g cm $^{-3}$ or $\lesssim 1$ cm $^{-3}$ need to be satisfied. A lower ISM density or higher mass-loss rate allows the wind to reach large distances.

A simple analytical treatment can give some useful insight. This is because a strict upper limit on the radial extent of the Wolf-Rayet wind can be obtained by computing the radius of the termination shock for a free expanding wind. The radius at the inner edge of the wind bubble can be found by balancing the wind ram pressure with the post-shock cavity pressure. For a star that loses mass at a rate $10^{-5} \dot{M}_{-5} M_{\odot} \text{ yr}^{-1}$ with a wind velocity $10^3 v_{w,3}$ km s $^{-1}$ in interstellar gas with density $10^0 n_{\text{ISM},0} \text{ cm}^{-3}$, we have an inner termination shock radius

$$r_t = 15 \dot{M}_{-5}^{3/10} v_{w,3}^{1/10} n_{\text{ISM},0}^{-3/10} t_6^{2/5} \text{ pc.} \quad (5)$$

where $10^6 t_6$ is the lifetime of the star in Myr. For sufficiently high \dot{M} or low n_{ISM} , the termination shock radius given in equation (6) can become larger than r_{\min} . This requires

$$\dot{M}_{-5}^{3/10} v_{w,3}^{1/10} n_{\text{ISM},0}^{-3/10} \gtrsim 3 \left(\frac{r_{\min}}{50 \text{ pc}} \right), \quad (6)$$

which shows that if the wind is specially massive ($\dot{M} \geq 10^{-4} M_{\odot} \text{ yr}^{-1}$) or the surrounding pressure is low ($n_{\text{ISM}} \leq 10^{-1} \text{ cm}^{-3}$), r_t falls above the radial range for which 99.99% of the C^{3+} ions are ionized. Interestingly, this low gas density is consistent with the low $N(\text{H I})$ observed in the host galaxy of GRB 021004, $\log N(\text{H I}) = 19.5 \pm 0.5$.

Here we consider possible scenarios that would help to alleviate the burden of forcing the wind out to beyond 30 pc.

We first consider the structured jet model discussed in Starling et al. (2005). These authors proposed that the ionization of circumstellar medium is dominated by a narrow and fast-moving jet, but the line of sight encompasses

We note that at this ionization level the spectra cannot rule out the possibility that the observed $N(\text{CIV})$ is due to gas at $r < 150$ pc, as it would only imply a total gas column for carbon of $\log N(\text{C}) \sim 15$ within this radius. It is therefore necessary to adopt a more stringent ionization threshold.

a wider and slower-moving jet through the wind, where the C^{3+} ions can survive at smaller distances to the burst. We consider this scenario unlikely for two main reasons. First, following this structured jet model, we expect to observe partial coverage of the absorption transitions along the line of sight. The CIV $\lambda 1548$ absorption line profile of Component 2 is completely saturated over the central $\Delta \lambda_{\text{obs}} = 0.8$ Å (Figure 7). We constrain the covering factor of C^{3+} ions along the line of sight at $f > 97\%$ at the 2- σ significance level. Second, light curve observations and modelling of GRBs 021004 and 050820 show that prompt emission of the GRB event contributes only a small fraction to the total ionizing photons (Vestrand et al. 2006; Lazzati et al. 2006). Therefore, the afterglow serves both as the background light probe and as the principle source of ionization of the circumstellar medium.

Next, we consider the possibility of a clumpy wind for a chemical composition that is characteristic of local Wolf-Rayet winds. Wolf-Rayet type stellar winds are found to have significant inhomogeneous spatial distributions and a chemical composition dominated by helium and carbon with little hydrogen (Crowther 2007). Dense clumps, located at smaller distances to the afterglow along the line of sight can in principle serve as a natural screen for shielding the clumps that are further away from the progenitor stars. The same model is commonly applied to study the presence of dusty tori in the vicinity of quasars (e.g. Königl & Kartje 1994).

To test whether a clumpy wind is a viable solution, we use the compressible turbulent hot-star outflow description of Moffat et al. (1994) as a working model, in which a simple scaling relation between the size, l_c , and density, ρ_c of the clumps is assumed to prevail: $\rho_c \propto l_c^{-1}$. What is more, Moffat et al. (1994) found that for Wolf-Rayet winds, a typical mass spectrum that follows $m_c^{-1.5}$ provides a reasonably good description of the emission line variations, where $m_c \propto \rho_c l_c^3$ is the mass of a clump. Taken together, the above scaling laws favor an asperous wind with clumps of varying size but constant column density and a mass spectrum dramatically raising to lower clump masses.

If full-scale turbulence really does prevail, the discrete clumps could in principle be usable to suppress a substantial fraction of the ionizing photon flux at $E_{\gamma} = h\nu > 64$ eV from the afterglow. To calculate the properties of the asperous wind, we first consider the following three constraints. First, the clump column density should be at least $N(\text{CIV}) \approx 1.5 \times 10^{18} \text{ cm}^{-2}$ so that $N(\text{CIV}) \times \sigma_{ph}(C^{3+}) = 1$ for suppressing a substantial fraction of the ionizing flux. Because the ionization potentials of He^+ and C^{3+} are very similar (see the inset of Figure 13)⁵, we treat He^+ and C^{3+} as the same particles in the photo-ionization process. This leads to a minimum gas clump gas column density of $N_g = N(\text{CIV}) \times (\text{C}/\text{He})^{-1} \approx 1.5 \times 10^{19} \text{ cm}^{-2}$ for Wolf-Rayet winds with $\text{C}/\text{He} = 0.1$. Second, the clump

⁵We note that photons of $E_{\text{phot}} > 350$ eV are energetic enough to remove electrons from the inner shell (K-shell states) and electrons in the outer shell (L-shell states) cascade down to fill the vacancy on time scales of a few fs (Schlachter et al. 2004). This explains the edge that appears at 350 eV in the inset of Figure 13. But because the afterglow radiation declines quickly with frequency ($\beta = -1$), ionization of C^{3+} due to the removal of a K-shell electron is limited to $\sim 10\%$.

size should be at least comparable to the apparent image size of the afterglow (e.g. Granot et al. 2005),

$$r_{\perp} = 2 \times 10^{16} E_{\text{iso},52}^{1/4} \dot{M}_{-5}^{1/4} v_{w,3}^{-1/4} [t_{\text{days}}/(1+z)]^{3/4} \text{ cm.} \quad (7)$$

This leads to a minimum clump mean gas density of $\rho_{c,\text{min}} \sim 750 \text{ cm}^{-3}$ and a minimum clump mass of $m_{c,\text{min}} \sim 4 \times 10^{-5} M_{\odot}$. Third, the total mass of the unshocked Wolf-Rayet wind sets a limit to the total number of available clumps at the smallest scale (note that given the assumed mass spectrum, the total mass of the outflow is dominated by the lower mass clumps, here assumed to be $\sim r_{\perp}$). In the unshocked wind, the mass within a radius r is $\dot{M} r/v_w$, which combined with the minimum clump mass estimate gives the maximum number of clumps of size $l_c \sim r_{\perp}$ within the $1/r^2$ wind:

$$n_c = 10^2 \dot{M}_{-5}^{7/4} v_{w,3}^{-7/4} \rho_{c,\text{min}}^{-1} r_{\text{pc}}. \quad (8)$$

The volume filling factor is thus given by

$$f_c = 3 \times 10^{-5} \dot{M}_{-5} v_{w,3}^{-1} \rho_{c,\text{min}}^{-1} r_{\text{pc}}^{-2}. \quad (9)$$

Whether a clumpy wind scenario is a viable solution for the survival of C^{3+} at $< 30 \text{ pc}$ depends on the number of clumps one can reasonably find along the line of sight to the afterglow. Adopting a total ionizing photon emission of $\phi_{\gamma} = 4 \times 10^{60}$ for GRB 021004 from Lazzati et al. (2006), we estimate a photon flux accumulated in time of $N_{\gamma} = 3 \times 10^{22} \text{ cm}^{-2}$ at $r = 1 \text{ pc}$. For $\rho_{c,\text{min}}$ one requires roughly

$$n_{\tau} = 2 \times 10^3 \rho_{c,\text{min}}^{-1} r_{\text{pc}}^{-2} \quad (10)$$

clumps to be present along the sightline to effectively absorb all the ionizing photons. It is therefore clear that a clumpy wind model fails, because there is simply not enough mass in the unshocked wind medium. A close inspection of the above requirements shows that for a fixed unshocked wind mass, altering $\rho_{c,\text{min}}$, r_{pc} or l_c (here assumed to be $\sim r_{\perp}$) fails to improve the situation. For example, in an extreme case scenario a single clump of $N_g = 1.5 \times 10^{22} \text{ cm}^{-2}$ (total clump mass of $0.05 M_{\odot}$ for $l_c = r_{\perp}$), at $r=1 \text{ pc}$ along the sightline is sufficient to absorb the large incident ionizing flux, but requires $\dot{M} \gg 10^{-2} M_{\odot} \text{ yr}^{-1}$ so that the probability of having one in front of the afterglow will be at least modest. We contend that a clumpy wind model is therefore an unlikely solution.

After a careful consideration of various scenario, we conclude that C^{3+} ions at $r < 30 \text{ pc}$ cannot survive the intense afterglow radiation field to impose an absorption feature in the afterglow spectrum.

5. SUMMARY AND CONCLUSIONS

We have collected a sample of five GRB afterglow spectra for an unbiased search of blue-shifted, high-velocity CIV absorbers at $|\Delta v| = 1000 - 5000 \text{ km s}^{-1}$ from the host redshift z_{GRB} . These absorbers (designated CIV₁₅) are candidate stellar wind features expected from a Wolf-Rayet progenitor of long-duration GRBs. Our sample, although small, is statistically unbiased, because it is assembled based on all available afterglow spectra suitable for our study without prior knowledge of the line-of-sight properties. We identify only one CIV₁₅ absorber at $\Delta v = -1500 \text{ km s}^{-1}$ from GRB 050730 and none along the rest of the sightlines to a $3\text{-}\sigma$ limit of $\text{EW} = 0.4 \text{ \AA}$ over a uniform $\delta v = 170 \text{ km s}^{-1}$ velocity resolution element.

Our search yields an estimate of 20% for the incidence of CIV₁₅ absorbers from the GRB host galaxies with a 68% confidence interval of 0–40%. This is consistent with what is expected for classical damped Ly α absorbers toward quasar sightlines. The result suggests that the majority of these CIV₁₅ absorbers originate in a foreground galaxy along the sightline.

We have also assembled an early sample based on GRB sightlines from earlier work, including GRBs 000926 (Castro et al. 2003), 021004 (Mirabal et al. 2003; Fiore et al. 2005), and 030323 (Vreeswijk et al. 2004). The sightline toward GRB 021004 is the only source that exhibits two CIV₁₅ absorbers at $\Delta v = -2675 \text{ km s}^{-1}$ (Component 1) and $\Delta v = -2900 \text{ km s}^{-1}$ (Component 2), respectively, as reported by previous authors. The CIV₁₅ absorbers found in the early sample offer additional insights for understanding their origin.

The presence of a saturated C II $\lambda 1334$ absorption and absence of C II* $\lambda 1335$ transition together allow us to rule out the possibility of Component 1 originating in the GRB progenitor environment. Our analysis shows that had the gas originated in the vicinity of the afterglow (i.e. at $r < 1 \text{ kpc}$), it would have been highly excited by the UV photons of the afterglow. Instead, Component 1 most likely originates in a foreground galaxy along the line of sight, which is supported by both the statistical expectation of the incidence of CIV absorbers and the presence of a faint galaxy at $0.3''$ away from the GRB host galaxy.

The lack of wind signatures for 80% of our statistical sample is understood as due to gas being photo-ionized by the intense UV radiation field of the afterglows. Our estimates show that ionizing photons from the afterglow can ionize C^{3+} to beyond 30 pc radius from the progenitor stars. We explore different scenarios that would allow C^{3+} to survive at close distances from the afterglow. We find based on a chemical composition C/He=0.1, typical of local Wolf-Rayet winds, a large density contrast in the wind can in principle provide necessary shielding for the C^{3+} ions, but but requires $\dot{M} \gg 10^{-2} M_{\odot} \text{ yr}^{-1}$ so that the probability of having one in front of the afterglow will be at least modest. We contend that a clumpy wind model is unlikely to be a viable scenario.

We thank N. Mirabal and P. Vreeswijk for sharing their spectra of GRB 021004 and GRB 030323. H.-W.C. acknowledges helpful discussions with A. J. van Marle, P. Crowther, J. Eldridge, C. Chin, and A. Königl. We thank Davide Lazzati and an anonymous referee for critical comments that helped to improve the paper. H.-W.C., JXP, and JSB acknowledge partial support from NASA grant NNG05GF55G. H.-W.C. was partially supported by NASA grant NNG06GC36G and NSF grant AST-0607510. E.R.-R acknowledges support from the John Bahcall Fellowship.

REFERENCES

- Adelberger, K. L. et al. 2005, ApJ, 629, 636
- Akerlof, C. et al. 1999, Nature, 398, 400
- Berger, E. et al. 2006, ApJ, 642, 979
- Bergeron, J. & Stasinska, G. 1986, A&A, 169 1
- Bernstein, R., Shectman, S. A., Gunnels, S. M., Mochnacki, S., & Athey, A. E. 2003, Proc. SPIE, 4841, 1694

- Bersier, D., et al. 2003, *ApJ*, 584, L43
- Bloom, J. S., Kulkarni, S. R., & Djorgovski, S. G. 2002, *AJ*, 123, 1111
- Castander, F. J. et al. 2002, *GCN Circ.* 1599
- Castro, S. et al. 2003, *ApJ*, 586, 128
- Castro-Tirado, A. J. et al. 2002, *GCN Circ.* 1635
- Cenko, S. B., Fox, D. B., & Berger, E. 2005, *GCN Circ.* 3944
- Chen, H.-W. & Prochaska, J. X. 2000, *ApJ*, 543, L9
- Chen, H.-W., Lanzetta, K. M., Webb, J. K., & Barcons, X. 2001, *ApJ*, 59, 654
- Chen, H.-W., Prochaska, J. X., Bloom, J. S., & Thompson, I. B. 2005, *ApJ*, 634, 25
- Chevalier, R. A., Li, Z.-Y., & Fransson, C. 2004, *ApJ*, 606, 369
- Chornock, R. & Filippenko, A. V. 2002, *GCN Circ.* 1605
- Christensen, L., Hjorth, J., & Gorosabel, J. 2004, *A&A*, 425, 913
- Cobb, B. E. & Bailyn, C. D. 2005, *GCN Circ.* 3708
- Cobb, B. E. 2006, *GCN Circ.* 4972
- Cowie, L. L., Songaila, A., Kim, T.-S., & Hu, E. M. 1995, *AJ*, 109, 1522
- Crowther, P. 2007, *ARA&A* in press (astro-ph/0610356)
- Damerdji, Y. et al. 2005, *GCN Circ.* 3741
- Della Valle, M. et al. 2006, *Nature* submitted (astro-ph/0608322)
- D'Odorico, S., Cristiani, S., Dekker, H., et al. 2000, in *SPIE* 4005, 121
- Eldridge, J. J., Genet, F., Daigne, F., & Mochkovitch, R. 2006, *MNRAS*, 367, 186
- Faber, S. M. et al. 2003, *SPIE*, 4841, 1657
- Falcone, A. D. et al. 2006, *GCN Circ.* 4966
- Fan, X. et al. 2001, *AJ*, 121, 54
- Ferland, G. J. et al. 1998, *PASP*, 110, 761
- Fiore, F. et al. 2005, *ApJ*, 624, 853
- Foley, R. J., Chen, H.-W., Bloom, J. S., & Prochaska, J. X. 2005, *GCN Circ.* 3949
- Fox, D. B. & Cenko, S. B. 2005, *GCN Circ.* 3829
- Fruchter, A. S. et al. 2006, *Nature*, 441, 463
- Fynbo, J. P. U. et al. 2005, *ApJ*, 633, 317
- Fynbo, J. P. U. et al. 2006a, *Nature* in press (astro-ph/0608313)
- Fynbo, J. P. U. et al. 2006b, *A&A*, 451, L47
- Gal-Yam, A. et al. 2006, *Nature* submitted (astro-ph/0608257)
- García-Segura, G., Langer, N., & Mac Low, M. M. 1996a, *A&A*, 316, 133
- Gilmore, A., Kilmartin, P., & Henden, A. 2003, *GCN Circ.* 1949
- Goad, M. et al. 2005, *GCN Circ.* 3942
- Granot, J., Ramirez-Ruiz, E., & Loeb, A. 2005, *ApJ*, 618, 413
- Graziani, C. et al. 2003, *GCN Circ.* 1956
- Gruendl, R. A., Chu, Y.-H., Dunne, B. C., & Points, S. D. 2000, *AJ*, 120, 2670
- Hamann, W.-R. & Koesterke, L. 1998, *A&A*, 335, 100
- Hammer, F., Flores, H., Schaefer, D., Dessauges-Zavadsky, M., Le Floch, E., & Puech, M. 2006, *A&A*, 454, 103
- Harrison, F. A. et al. 2001, *ApJ*, 559, 123
- Hjorth, J. et al. 2003, *Nature*, 423, 847
- Holland, S. T. et al. 2003, *AJ*, 125, 2291
- Holland, S. T. et al. 2005, *GCN Circ.* 3704
- Hurley, K. et al. 2000, *GCN Circ.* 801
- Jakobsson, P. et al. 2006, *A&A Letters* in press (astro-ph/0609450)
- Klose, S. et al. 2004, *AJ*, 128, 1942
- Klotz, A., Boer, M., & Atteia, J. L. 2005, *GCN Circ.* 3720
- Königl, A. & Kartje, J. F. 1994, *ApJ*, 434, 446
- Lazzati, D., Rosalba, P., Flasher, J., Dwarkadas, V., & Fiore, F. 2006, *MNRAS* in press (astro-ph/0608437)
- Li, Z.-Y. & Chevalier, R. A. 2003, *ApJ*, 589, L69
- Li, W. 2005, *GCN Circ.* 3945
- Lopez, S., Reimers, D., Rauch, M., Sargent, W. L. W., & Smette, A. 1999, *ApJ*, 513, L598
- MacFadyen, A. I. & Woosley, S. E. 1999, *ApJ*, 524, 262
- Mirabal, N. et al. 2003, *ApJ*, 595, 935
- Moffat, A. F. J., Lepine, S., Henriksen, R. N., & Robert, C. 1994, *Ap&SS*, 216, 55
- Møller, P. et al. 2002, *A&A*, 396, L21
- Nahar, S. N. & Pradhan, A. K. 1997, *A&AS*, 111, 339
- Niedzielski, A., & Rochowicz, K. 1994, *A&AS*, 108, 669
- Oke, J. B., et al. 1995, *PASP*, 107, 375
- Page, M. et al. 2005, *GCN Circ.* 3830
- Panaitescu, A., & Kumar, P. 2000, *ApJ*, 543, 66
- Pandey, S. B., et al. 2003, *Bull. Astron. Soc. India*, 31, 19
- Perna, R., & Lazzati, D. 2002, *ApJ*, 580, 261
- Petitjean, P. & Bergeron, J. 1994, *A&A*, 283, 759
- Prochaska, J. X. et al. 2005, *GCN Circ.* 3971
- Prochaska, J. X., Chen, H.-W., & Bloom, J. S. 2006, *ApJ* in press
- Prochaska, J. X., Chen, H.-W., Bloom, J. S. et al. 2006, *ApJS*, in press
- Prochaska, J. X. et al. 2007, *ApJS*, submitted
- Prochter, G. et al. 2006, *ApJ*, 648, 93
- Ramirez-Ruiz, E., Dray, L., Madau, P., & Tout, C. A. 2001, *MNRAS*, 327, 829
- Ramirez-Ruiz, E., García-Segura, G., Salmonson, J. D., & Pérez-Rendón, B. 2005, *ApJ*, 631, 435
- Rykoff, E. S. et al. 2005, *GCN Circ.* 4251
- Sakamoto, T., et al. 2005, *ApJ*, 629, 311
- Sakamoto, T. et al. 2005, *GCN Circ.* 4248
- Salamanca, I. et al. 2002, *GCN Circ.* 1611
- Sargent, W. L. W., Boksenberg, A., & Steidel, C. C. 1988, *ApJS*, 68, 539
- Sari, R., Piran, T., & Narayan, R. 1998, *ApJ*, 497, L17
- Savage, B. D. & Sembach, K. R. 1991, *ApJ*, 379, 245
- Schady, P. & Falcone, A. D. 2006, *GCN Circ.* 4978
- Schaefer, B. et al. 2003, *ApJ*, 588, 387
- Schlachter, A. S. et al. 2004, *J. Phys. B: At. Mol. Opt. Phys.*, 37, L103
- Scott, J., Bechtold, J., Dobrzycki, A., & Kulkarni, V. P. 2000, *ApJS*, 130, 67
- Sheinis, A. I. et al. 2002, *PASP*, 114, 851
- Shin, M.-S. et al., *ApJ* submitted (astro-ph/0608327)
- Shirasaki, Y. et al. 2002, *GCN Circ.* 1565
- Silva, A. I. & Viegas, S. M. 2002, *MNRAS*, 329, 135
- Simcoe, R. A. 2006, *ApJ* submitted (astro-ph/0605710)
- Songaila, A. 2006, *AJ*, 131, 24
- Stanek, K. Z. et al. 2003, *ApJ*, 591, L17
- Starling, R. L. C. et al. 2005, *MNRAS*, 360, 305
- Steidel, C. C. 1992, *PASP*, 104, 843
- Torii, K. 2005, *GCN Circ.* 3943
- Uemura, M., Kato, T., Ishioka, R., & Yamaoka, H. 2003, *PASJ*, 55, L 31
- van der Hucht, K. A. 2001, *New Astronomy Reviews*, 45, 135
- van Marle, A. J., Langer, N., García-Segura, G. 2005, *A&A*, 444, 837
- van Marle, A. J., Langer, N., Achterberg, A., & García-Segura, G. 2006, *A&A* in press (astro-ph/0605698)
- Verner, D. A. & Yakovlev, D. G. 1995, *A&AS*, 109, 125
- Verner, D. A., Ferland, G. J., Korista, K. T., & Yakovlev, D. G. 1996, *ApJ*, 465, 487
- Vestrand, W. T. et al. 2006, *Nature*, 442, 172
- Vogt, S. S., et al. 1994, *Proc. SPIE*, 2198, 362
- Vreeswijk, P. et al. 2004, *A&A*, 419, 927
- Vreeswijk, P. et al. 2006, submitted to *A&A* (astro-ph/0611690)
- Weatherley, S. J., Warren, S. J., Møller, P., Fall, S. M., Fynbo, J. U., & Croom, S. M. 2005, *MNRAS*, 358, 985
- Wijers, R. A. M. J. 2001, in *Gamma Ray Bursts in the Afterglow Era*, ed. E. Costa, F. Frontera, & J. Hjorth (Berlin: Springer), 306
- Willis, A. J., Crowther, P. A., Fullerton, A. W., Hutchings, J. B., Sonneborn, G., Brownsberger, K., Massa, D. L., & Walborn, N. R. 2004, *ApJS*, 154, 651
- Woosley, S. E. & Bloom, J. S. 2007, *ARA&A* in press (astro-ph/0609142)

TABLE 1
SUMMARY OF ABSORPTION-LINE PROPERTIES

Field	$E_{\text{iso}}(\times 10^{53} \text{ ergs})^{\text{a}}$	z_{GRB}	$\log N(\text{H I})$	$[\frac{\text{M}}{\text{H}}]_{\text{ISM}}$	$-\Delta v_{\text{CIV}}^{\text{max}}$	$t_{\text{obs}}^{\text{spec}} \text{ (hr)}$
The Statistical Sample						
GRB 050730 ...	1.2 ± 0.2	3.968	22.15 ± 0.05	-2.0 ± 0.1	1500 ^b	(4.0 – 5.7)
GRB 050820A .	2.0 ± 0.4	2.615	21.00 ± 0.10	-0.6 ± 0.1	250	(0.9 – 1.4)
GRB 050908 ...	0.11 ± 0.01	3.344	19.2 ± 0.2	~ -0.9	200	$(3.7 - 4.3)/(7.7 - 8.4)^{\text{c}}$
GRB 051111 ...	0.62 ± 0.05	1.549	> 20.3	< 0.9	200	(2.6 – 3.3)
GRB 060418 ...	0.67 ± 0.05	1.490	> 20.3	< 0.0	250	(0.5 – 2.3)
The Early Sample						
GRB 000926 ...	2.4 ± 0.8	2.038	21.3 ± 0.2	-0.17 ± 0.05	250	(29.1 – 30.5)
GRB 021004 ...	0.5 ± 0.1	2.328	19.6 ± 0.3	-1.3 ± 0.5	2900	(13.6 – 17.1)
GRB 030323 ...	0.3 ± 0.1	3.372	21.90 ± 0.07	-1.0 ± 0.2	200	(57.2 – 61.2)

^aGRBs 050730, 050820A, 050908, 051111 & 060418: Butler et al. 2006, in preparation. GRB 000926: Harrison et al. 2001; GRBs 021004 & 030323: Sakamoto et al. 2005.

^bContaminated by the atmosphere A-band absorption.

^cSpectra obtained using GMOS on the Gemini North telescope and DEIMOS on the Keck telescope, respectively. See descriptions in § 2.6.

TABLE 2
IONIC COLUMN DENSITIES OF “HIGH-VELOCITY” GAS TOWARD GRB 021004^{a,b}

Transition	component 1 $\Delta v = -2675 \text{ km s}^{-1}$	component 2 $\Delta v = -2900 \text{ km s}^{-1}$
CIV 1550	14.07 ± 0.02	> 14.72
CII 1334	> 14.46	13.62 ± 0.04
SiIV 1402	contaminated	13.8 ± 0.3
SiII 1526	13.42 ± 0.04	< 12.92

^aWe note that Fiore et al. (2005) presented independent measurements for these transitions. However, they did not account for the saturation of strong lines and presented lower limits as in measurements with errors.

^aErrors presented here account for only statistical errors. Uncertainties due to continuum fitting contribute to ~ 0.05 dex.

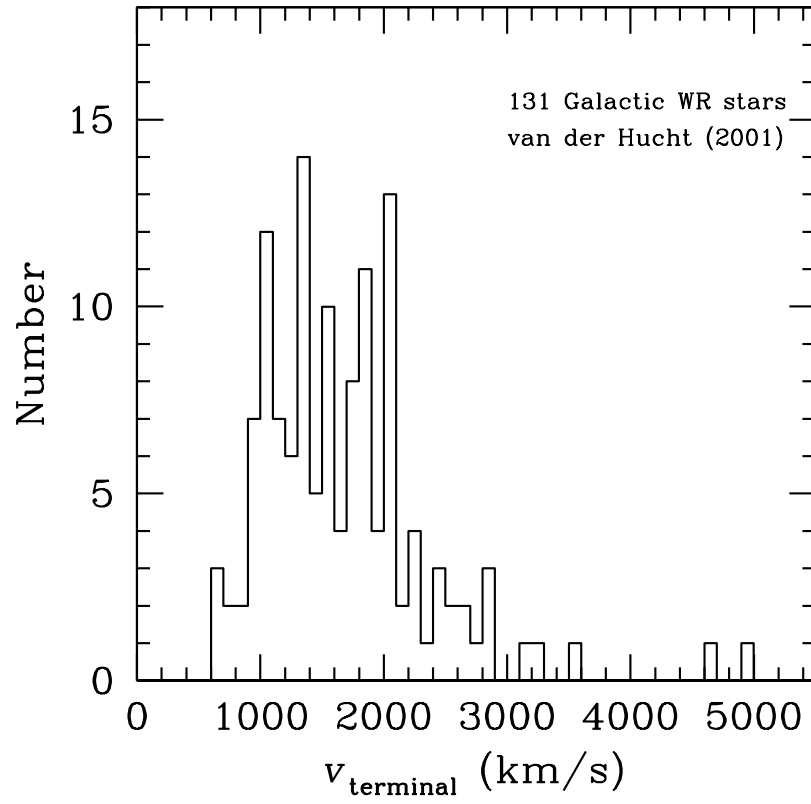


FIG. 1.— Number counts of Galactic Wolf-Rayet stars versus terminal wind velocity as determined from P-Cygni profiles of absorption lines like C IV λ 1550 (van der Hucht 2001).

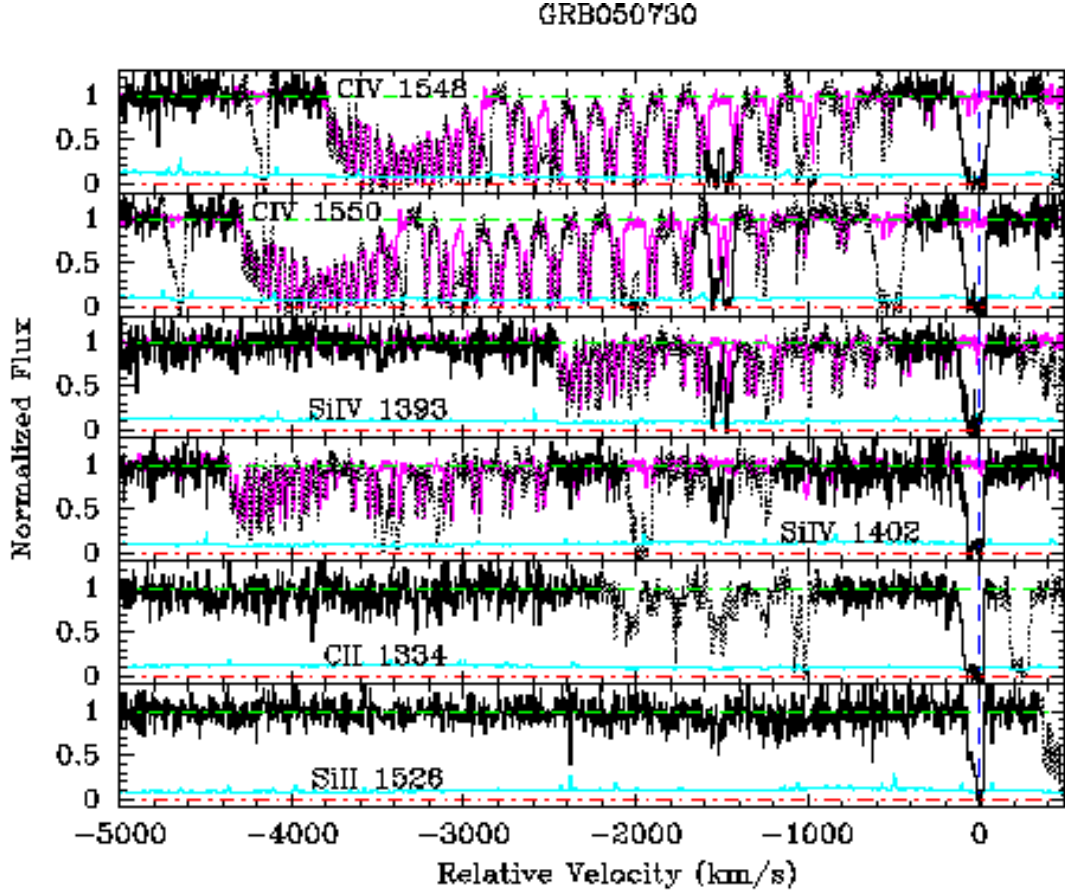


FIG. 2.— Absorption profiles of CIV $\lambda\lambda$ 1548, 1550, SiIV $\lambda\lambda$ 1393, 1402, CII λ 1334, and SiII λ 1526 observed in the host of GRB 050730. Zero relative velocity corresponds to $z = 3.96855$. Over the velocity interval from $\Delta v = -5000 \text{ km s}^{-1}$ through $\Delta v = -1000 \text{ km s}^{-1}$, we detect one blue-shifted CIV and SiIV absorber at $\Delta v \approx -1500 \text{ km s}^{-1}$. The CIV features are contaminated by the atmosphere A-band absorption forest. Although we are unable to obtain an accurate measurement of the column density of the C^{3+} ions, we place a lower limit to the rest-frame absorption equivalent width of $\text{EW}(\lambda 1550) > 0.36 \text{ \AA}$. The detection of the CIV absorption doublet is robust from the comparison with a quasar spectrum (the magenta curve) obtained using the same instrument at the same observation site (PKS2000; Prochter et al. 2007, in preparation). For SiIV, we measure $\log N(\text{SiIV}) = 13.9 \pm 0.1$. The contaminating absorption features are dotted out. The dashed-dotted lines indicate the normalized continuum and zero level for guide. The $1\text{-}\sigma$ error array is shown in thin, cyan line. Zero relative velocity corresponds to $z = 2.32897$.

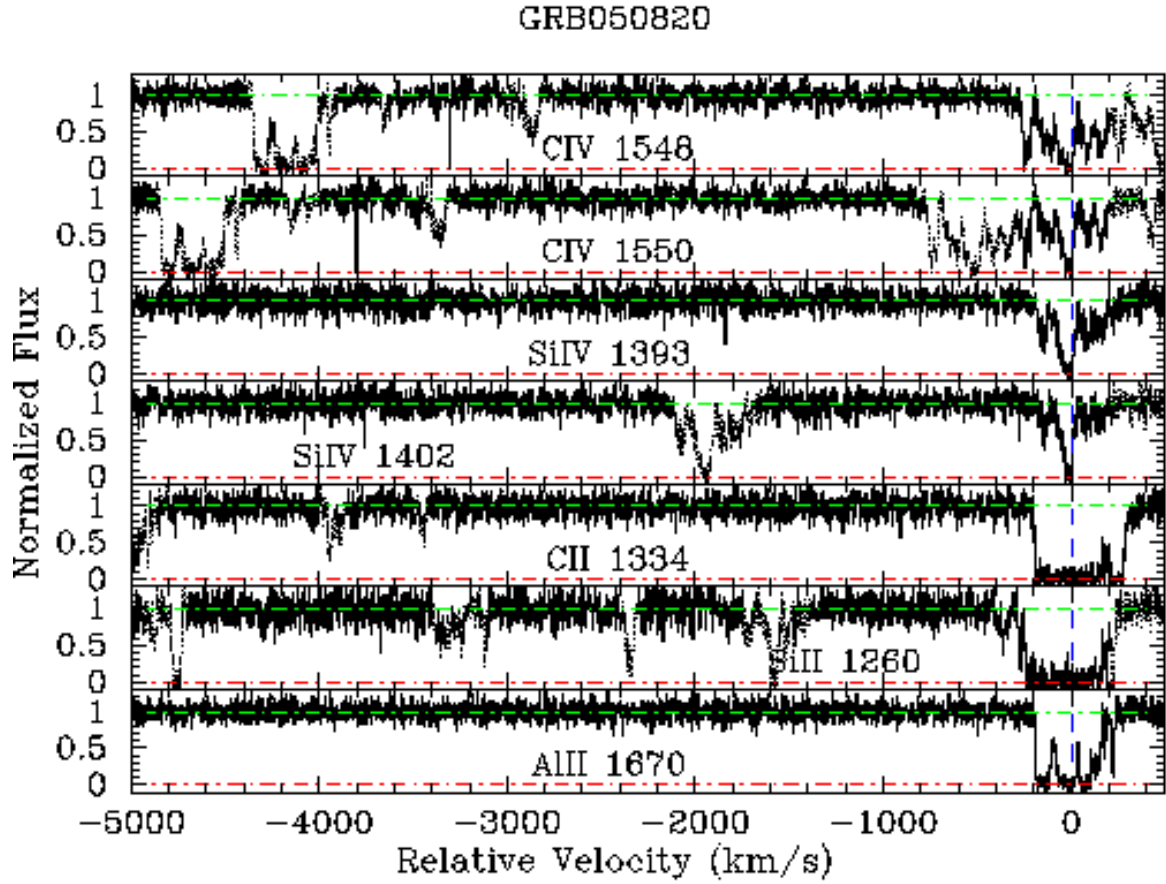


FIG. 3.— Absorption profiles of CIV $\lambda\lambda$ 1548,1550, SiIV $\lambda\lambda$ 1393,1402, CII λ 1334, SiII λ 1260, and AlII λ 1670 observed in the host of GRB 050820. Zero relative velocity corresponds to $z = 2.6147$. Over the velocity interval from $\Delta v = -5000 \text{ km s}^{-1}$ through $\Delta v = -1000 \text{ km s}^{-1}$, we do not detect additional CIV features with a $3\text{-}\sigma$ upper limit in the rest-frame absorption equivalent width of $\text{EW} = 0.2 \text{ \AA}$ over the spectral resolution element of $\delta v = 7.5 \text{ km s}^{-1}$.

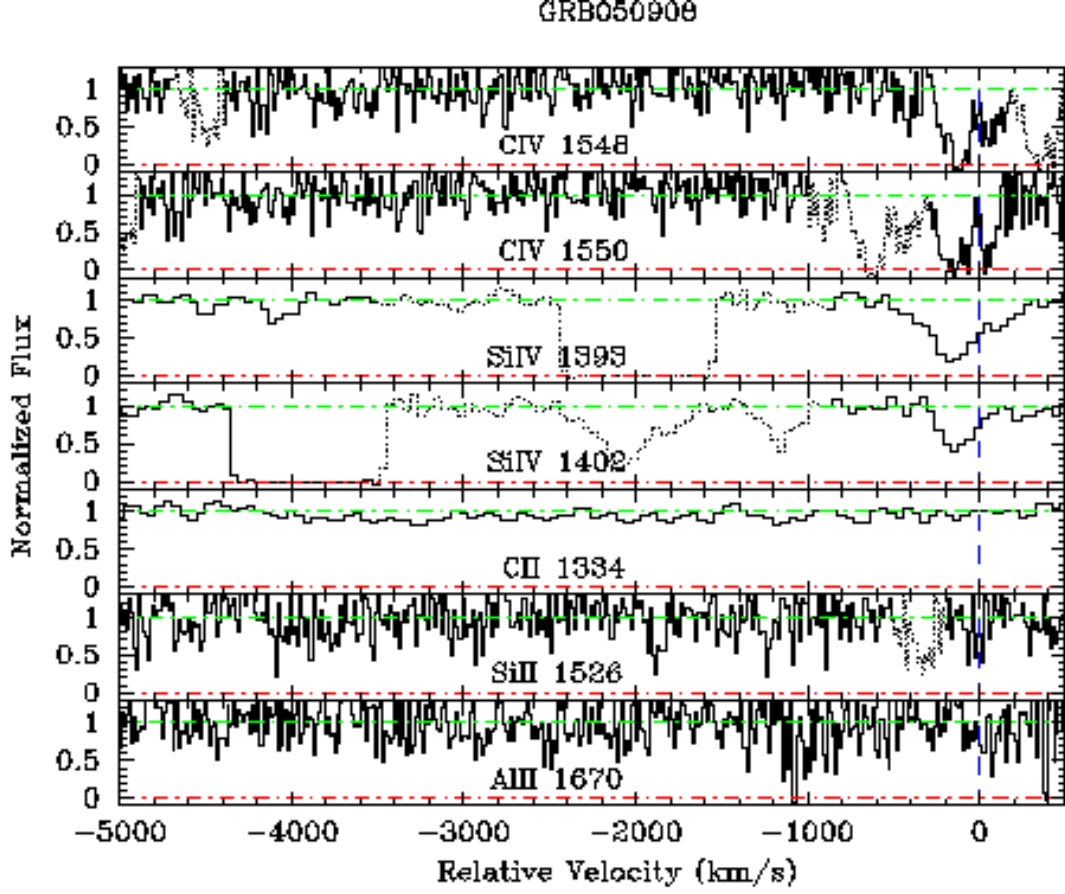


FIG. 4.— Absorption profiles of CIV $\lambda\lambda$ 1548, 1550, SiIV $\lambda\lambda$ 1393, 1402, CII λ 1334, SiII λ 1526, and AlII λ 1670 observed in the host of GRB050908. Zero relative velocity corresponds to $z = 3.344$. High-resolution data were taken using DEIMOS on the Keck II telescope and low-resolution data were taken using GMOS on the Gemini north telescope, which had non-contiguous spectral coverage due to chip gaps in the camera. One of the chip gaps is apparent in the SiIV doublet transitions. Over the velocity interval from $\Delta v = -5000 \text{ km s}^{-1}$ through $\Delta v = -1000 \text{ km s}^{-1}$, we do not detect additional CIV features with a $3\text{-}\sigma$ upper limit in the rest-frame absorption equivalent width of $\text{EW}(\lambda 1548) = 0.28 \text{ \AA}$ over the spectral resolution element of $\delta v = 40 \text{ km s}^{-1}$.

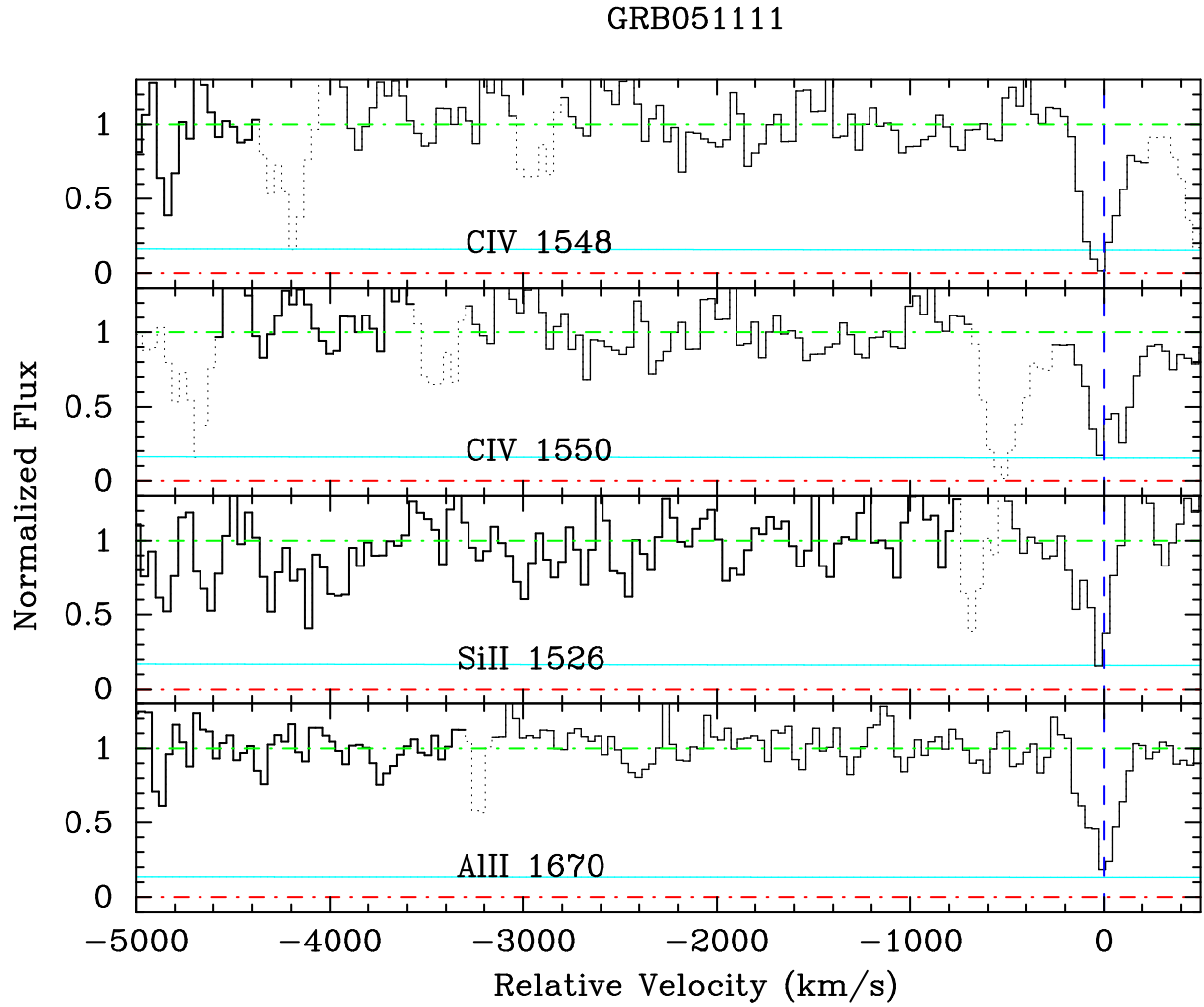


FIG. 5.— Absorption profiles of CIV $\lambda\lambda 1548, 1550$, SiII $\lambda 1526$, and AlII $\lambda 1670$ observed in the host of GRB051111 with GMOS on Gemini-N. Zero relative velocity corresponds to $z = 1.54948$. Over the velocity interval from $\Delta v = -5000 \text{ km s}^{-1}$ through $\Delta v = -1000 \text{ km s}^{-1}$, we do not detect additional CIV features with a $3\text{-}\sigma$ upper limit in the rest-frame absorption equivalent width of $\text{EW}(\lambda 1548) = 0.37 \text{ \AA}$ over the spectral resolution element of $\delta v = 170 \text{ km s}^{-1}$.

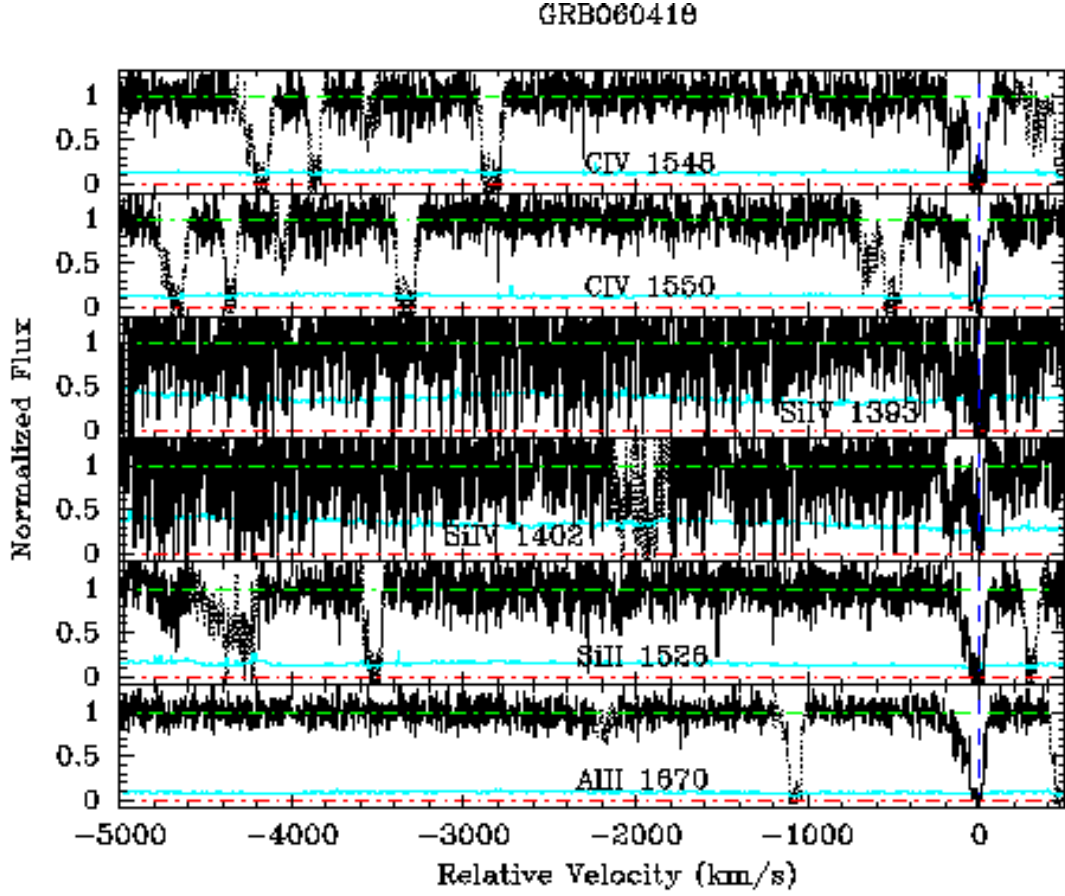


FIG. 6.— Absorption profiles of CIV $\lambda\lambda$ 1548, 1550, SiIV $\lambda\lambda$ 1393, 1402, CII λ 1334, SiII λ 1526, and AlII λ 1670 observed in the host of GRB 060418. Zero relative velocity corresponds to $z = 1.4901$. Over the velocity interval from $\Delta v = -5000 \text{ km s}^{-1}$ through $\Delta v = -1000 \text{ km s}^{-1}$, we do not detect additional CIV features with a $3\text{-}\sigma$ upper limit in the rest-frame absorption equivalent width of $\text{EW}(\lambda 1548) = 0.36 \text{ \AA}$ over the spectral resolution element of $\delta v = 12 \text{ km s}^{-1}$.

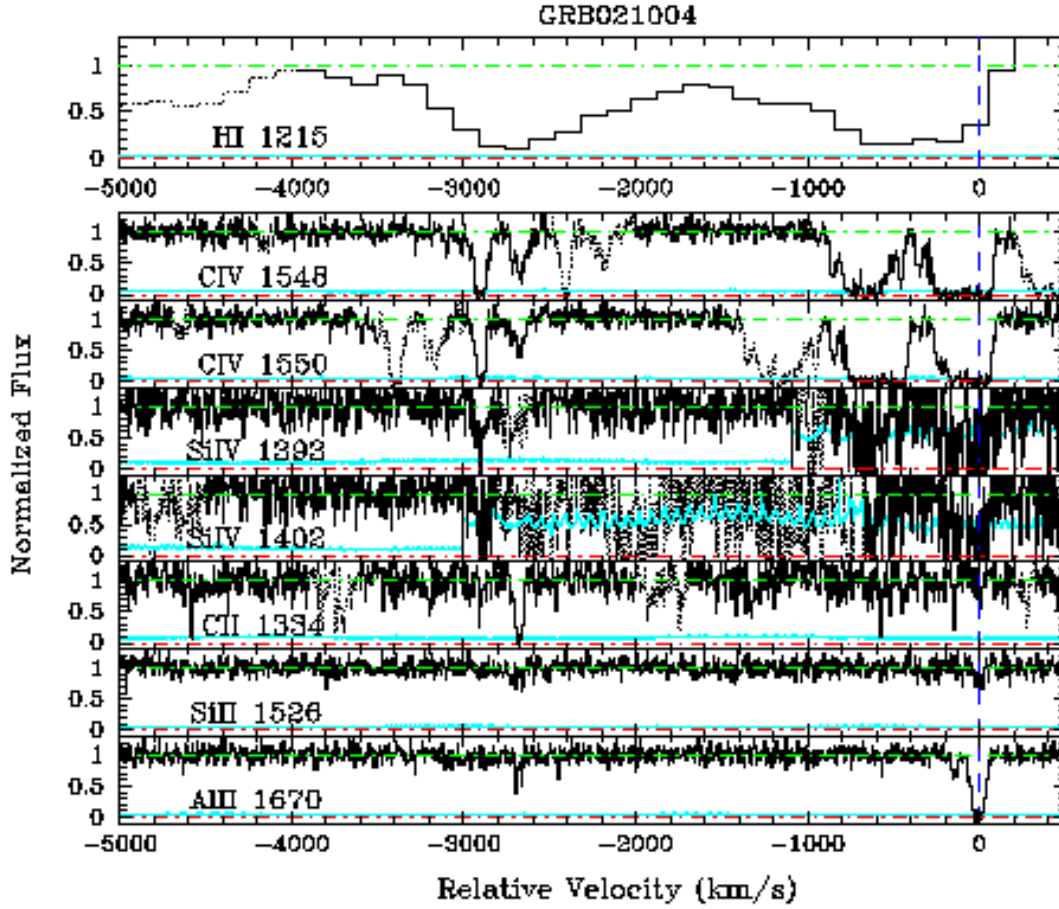


FIG. 7.— Absorption profiles of HI Ly α λ 1215, CIV $\lambda\lambda$ 1548, 1550, SiIV $\lambda\lambda$ 1393, 1402, CII λ 1334, SiII λ 1526, and AlII λ 1670 observed in the host of GRB 021004. The same as Figure 2, where contaminating absorption features are dotted out. The dashed-dotted lines indicate the normalized continuum and zero level for guide. The $1-\sigma$ error array is shown in thin, cyan line. Zero relative velocity corresponds to $z = 2.32897$. Over the velocity interval from $\Delta v = -5000 \text{ km s}^{-1}$ through $\Delta v = -1000 \text{ km s}^{-1}$, we identify two absorption components at $\Delta v = -2675 \text{ km s}^{-1}$ and $\Delta v = -2900 \text{ km s}^{-1}$, respectively.

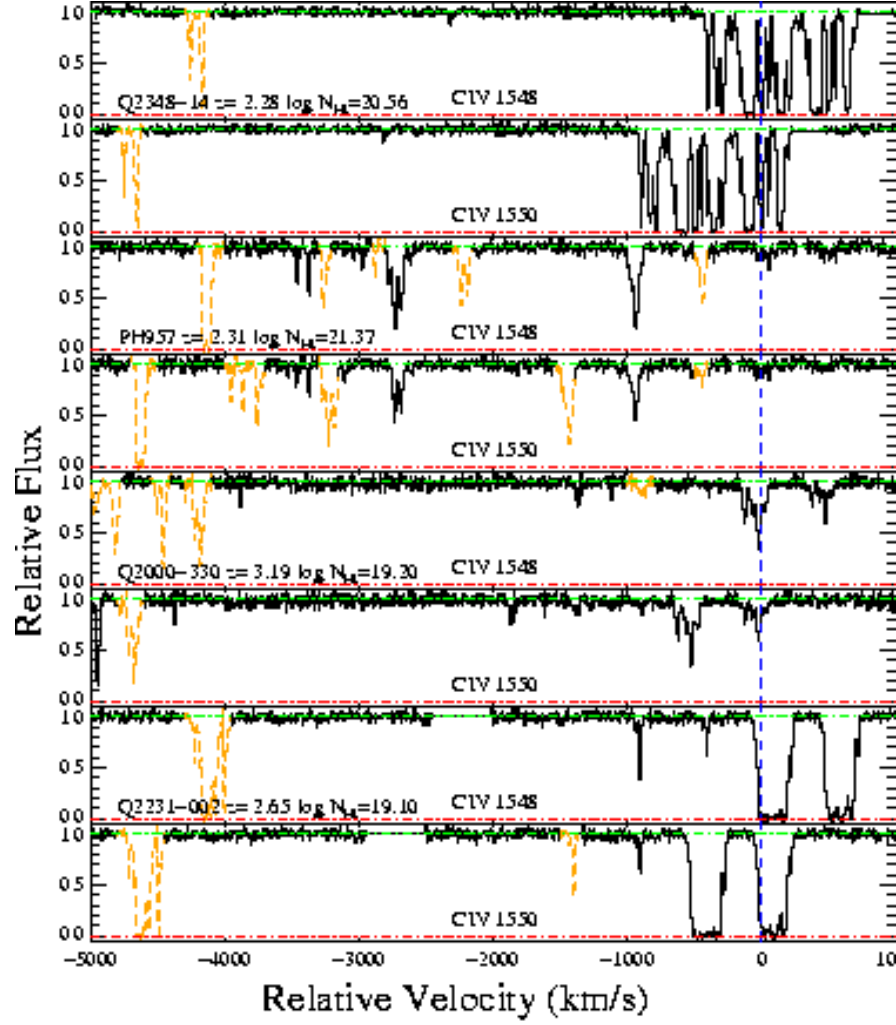


FIG. 8.— A sample of four strong intervening $\text{Ly}\alpha$ absorbers, two DLAs and two super Lyman limit systems, at $2.2 < z < 3.2$ toward quasar lines of sight. Contaminating features have been dotted out. These are part of the 53 quasar sightlines from the Keck/UCSD High Resolution database (Prochaska et al. 2007). We adopt this sample of 53 quasars as a control sample for estimating the statistical significance of possible “over-abundance” of CIV_{15} absorbers.

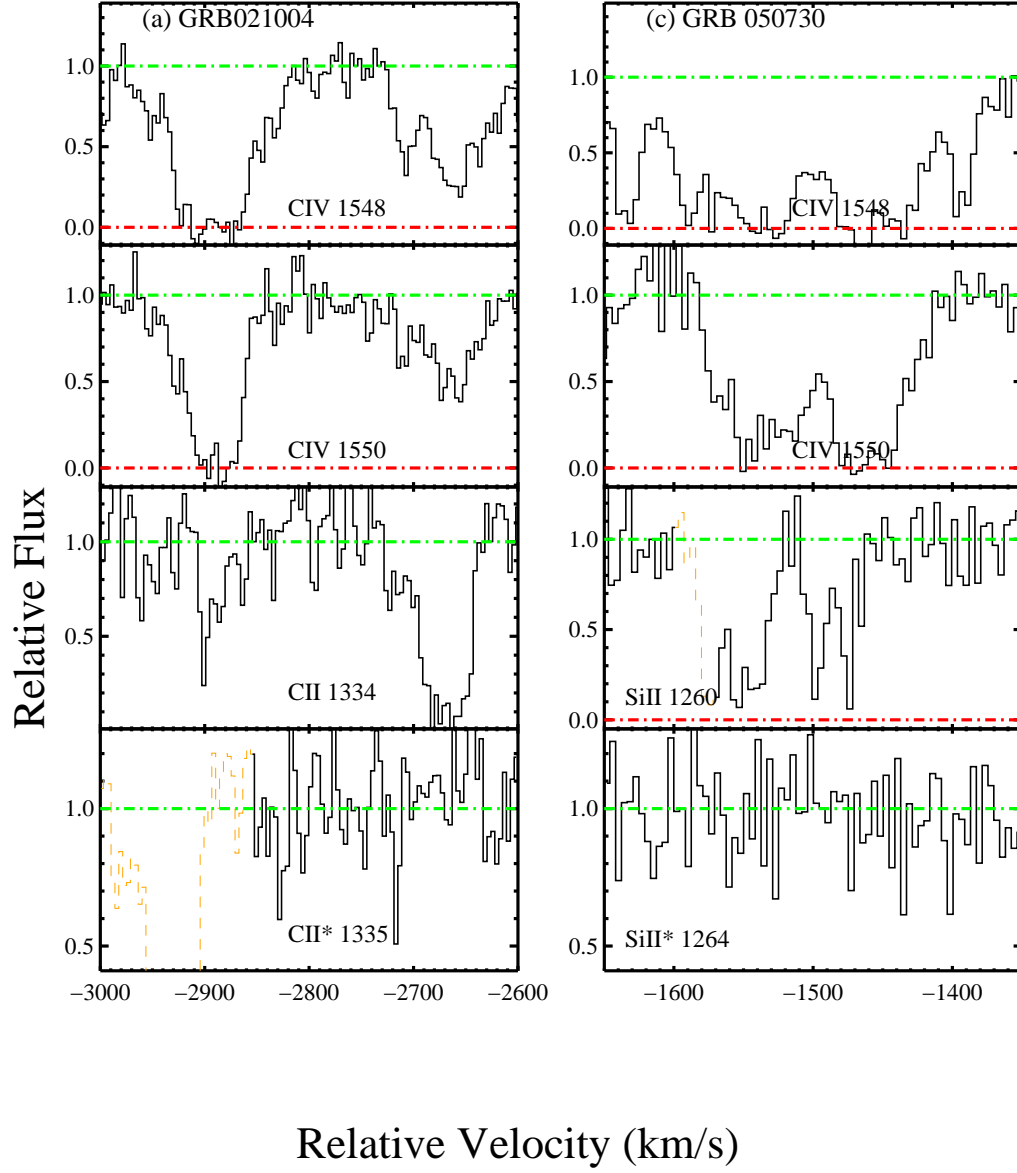


FIG. 9.— Velocity profiles for the CIV₁₅ absorbers from GRB 021004 (left panels) and from GRB 050730 (right panels). We also present the low-ion transitions of CII λ 1334 and SiII λ 1260 for GRB 021004 and GRB 050730, respectively, together with their associated fine-structure transitions. No excited transitions are detected in either of the sources.

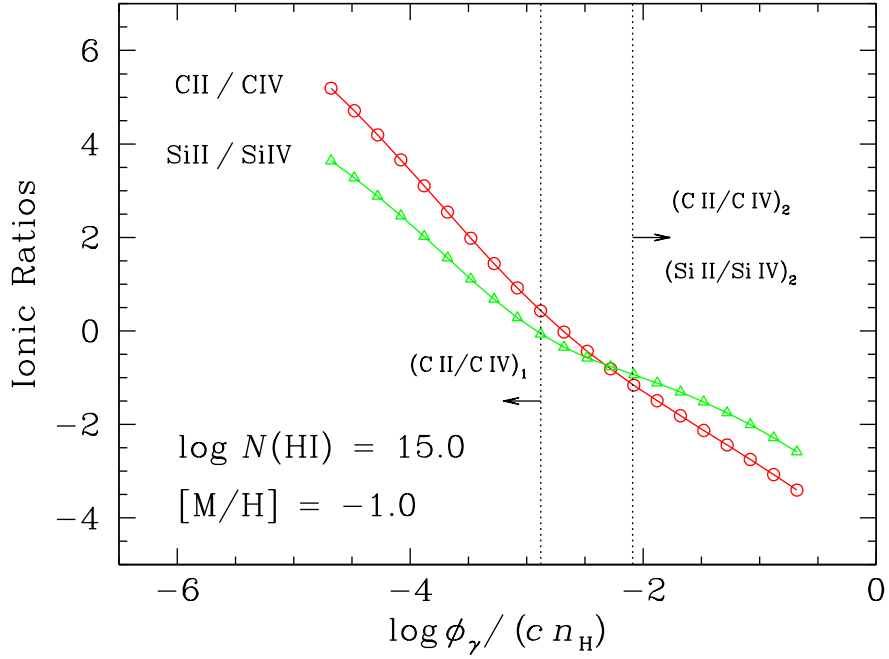


FIG. 10.— Expected ionic abundance ratios versus the ionization parameter $U \equiv \phi_\gamma / c n_H$. The expectations are calculated using the Cloudy software (Ferland et al. 1998; version 06.02) for clouds of plane parallel geometry and under photo-ionization equilibrium. We have assumed a metallicity of 0.1 solar and $\log N(\text{H I}) = 15$ and adopted the background radiation field of Haardt & Madau (2006 in preparation) that includes ionizing photons from both quasars and starburst galaxies. Constraints on the ionization parameter based on the observed relative abundances between different ionization stages are shown in vertical lines for the two components toward GRB 021004.

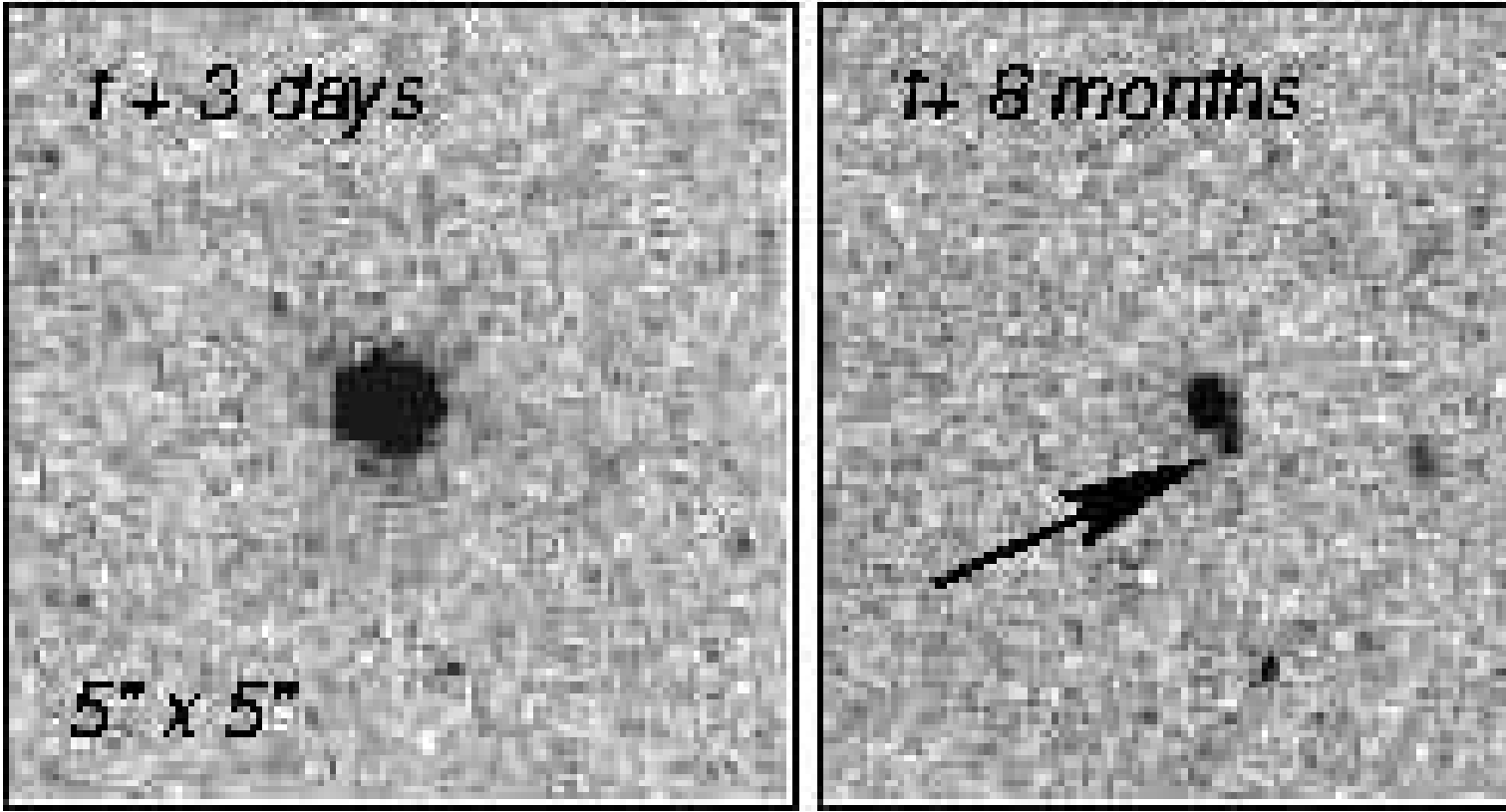


FIG. 11.— Images of the field surrounding GRB 021004, obtained using HST/ACS with the F606W filter three days (left panel) and eight months (right panel) after the trigger. The second epoch image (right panel), obtained when the optical afterglow had faded, clearly shows a faint companion (pointed by the arrow) next to the host galaxies at the center of the frame.

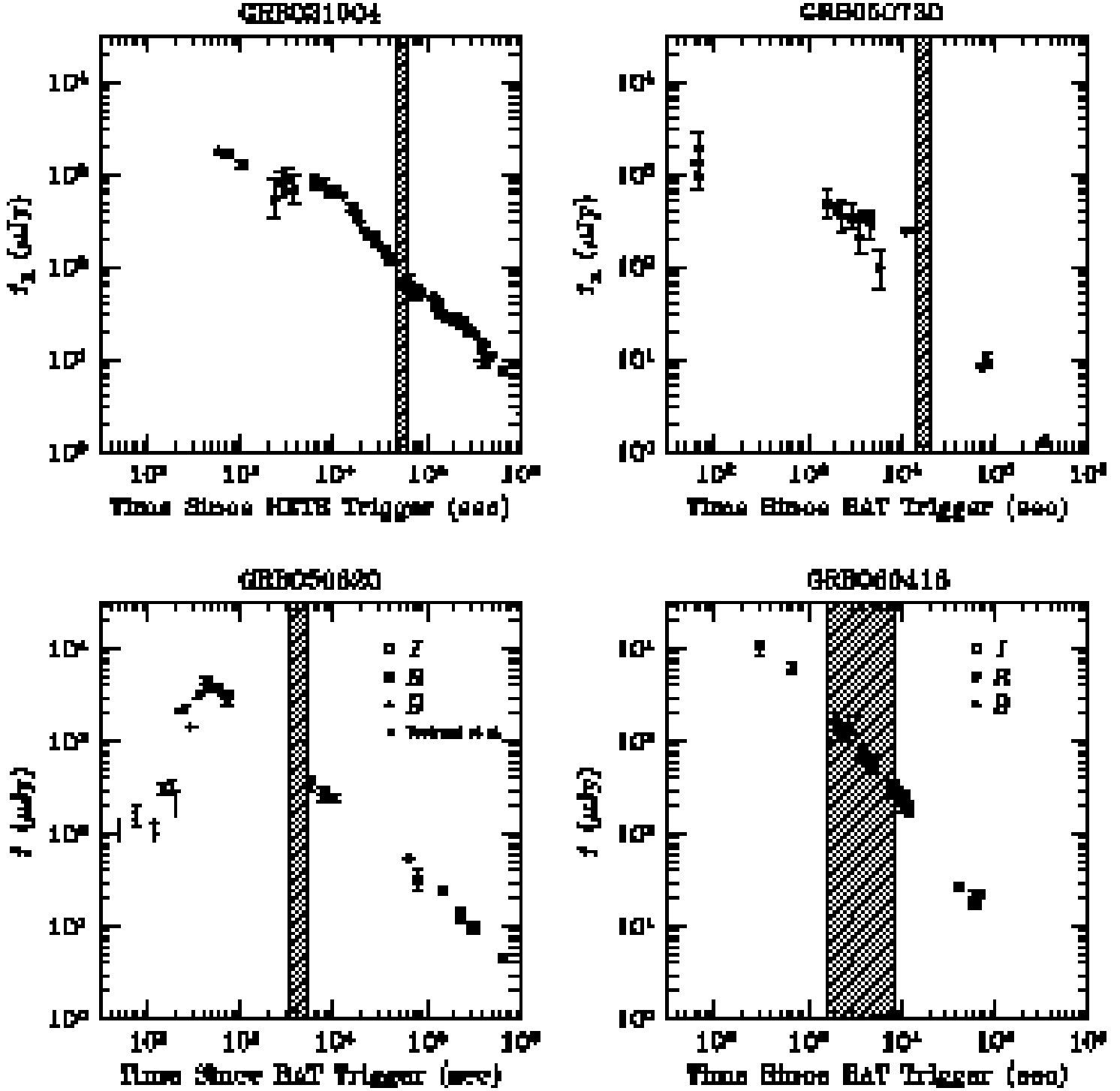


FIG. 12.— Optical light curves of GRBs 021004, 050730, 050820, and 060418, for which photometric measurements from < 10 minutes after the initial burst are available. The vertical shaded regions indicate the period when the spectroscopic data were taken. The light curves of GRBs 021004 and 050730 are based on R -band observations alone, while the light curves of GRBs 050820 and 060418 include observations in the B , R , and I bands. We have corrected for the Galactic extinction, when combining photometry from different bandpasses with $E(B - V) = 0.04$ toward GRB 050820 and $E(B - V) = 0.22$ toward GRB 060418. Observations of GRB 021004 were taken from Holland et al. (2003) and Uemura et al. (2003). Observations of GRB 050730 were taken from Klotz et al. (2005) and Damerdjian et al. (2005). Observations of GRB 050820 were taken from Vestrand et al. (2006). Observations of GRB 060418 were taken from Schady & Falcone (2006) and Cobb (2006).

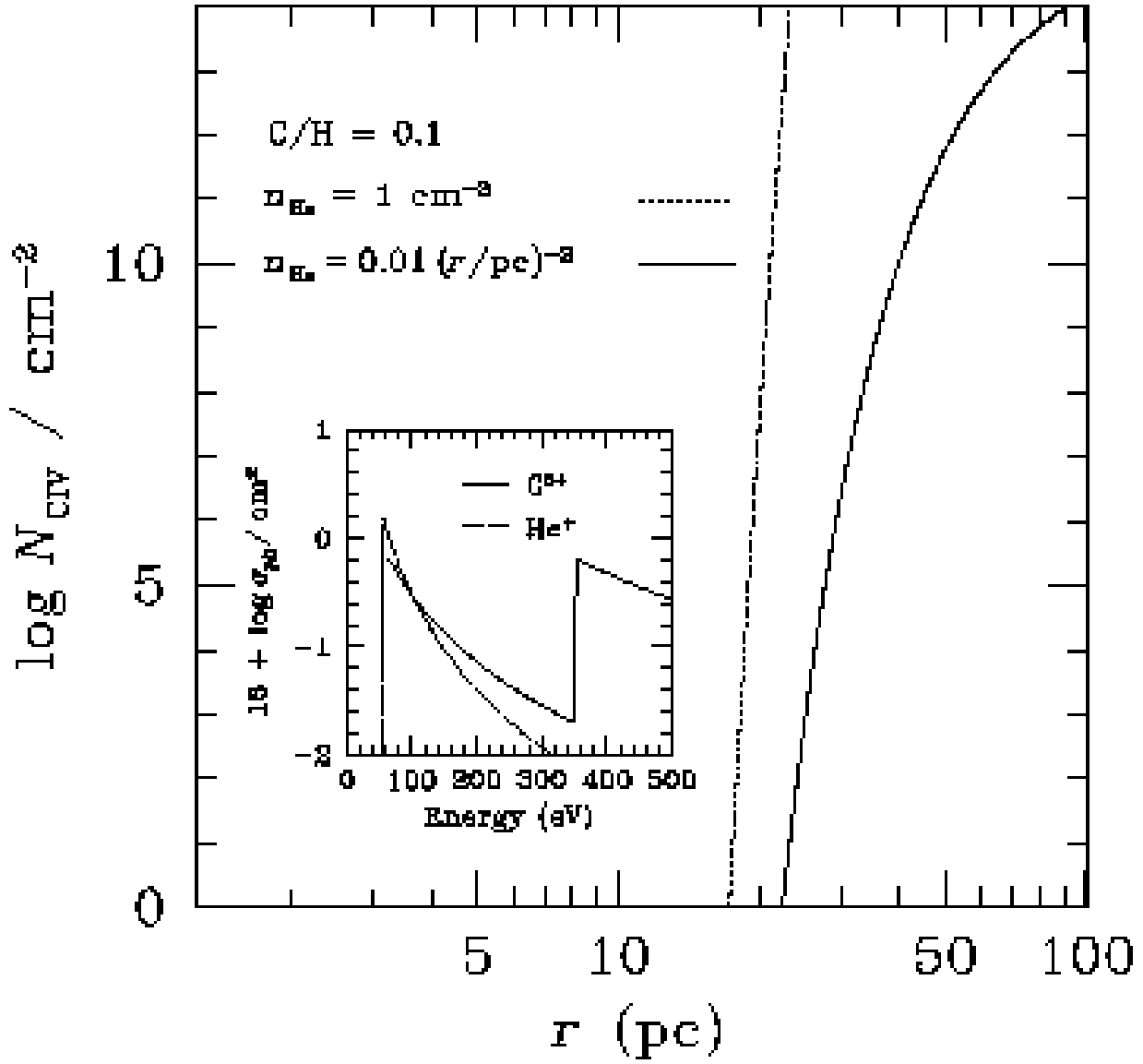


FIG. 13.— Estimated $N(\text{CIV})$ versus distance to the afterglow in the presence of He^+ for two different density profiles. The inset shows the photo-ionization cross sections of He^+ and C^{3+} versus photon energy. The curves are calculated according to Verner & Yakovlev (1995) and Verner et al. (1996).